

Reply to the review of P.P. Tans

The authors would like to thank P.P. Tans for his valuable comments. In the following, referee's comments are given in bold and author's responses in plain text. Suggested new text is quoted in italics together with page and line numbers.

General comments: The authors performed a series of experiments to learn more about wall effects in aluminum and steel high pressure gas cylinders at different pressures and temperatures. The trace gases considered are CO₂, CH₄, CO and low amounts of water vapor in air. In order to increase wall effects they chose to make special small cylinders with a higher wall to volume ratio. Additional advantages are that one has easy access to the interior surface and it is also easier to control the temperature of the small cylinders in a small oven. However, it is a significant disadvantage that their internal surface may not be the same as in the larger Luxfer cylinders that are almost universally used to distribute calibration mixtures for high precision greenhouse gas measurements. Luxfer claims that it has a proprietary version of the 6061 alloy, its manufacturing process is very different, and the surface treatment of the author's cylinders is also different from Luxfer's. The smallest high pressure Luxfer cylinder has a volume of only~700 cc; It is a pity that they did not include it in their experiments. The author's steel cylinder offers a comparison because its wall effects are different from aluminum. Stainless steel is often used for trace gases other than the main greenhouse gases.

We appreciate our reviewer's valuable comments and ideas. Unfortunately, we were not aware of the availability of the small size Luxfer cylinders. The small cylinder from Luxfer would indeed be a very valuable addition to these measurements, unfortunately we won't be able to conduct more measurements within the presented study. However, in our study, we put a strong focus on being able to open and close the cylinders because these measurement chambers were constructed primarily for material studies (Satar et al., 2019).

The smaller volume enables to fill and measure the cylinders easily. The surface of the small cylinder $A_{\text{cyl}} = 0.18 \text{ m}^2$ which results in a surface to volume ratio of 35.7. Therefore, we estimate the small cylinders to be more susceptible to adsorption by about 40 % than the 29.5 L Luxfer cylinders. It is also crucial to note that the real surface is expected to be significantly larger than the geometric surface area depending on the surface roughness.

We will add the following to the discussion:

"In order to understand the differences between the constructed cylinders and the Luxfer aluminum cylinder, measurements with a Luxfer cylinder of a similar size (5 L) and pressure ranges (up to 30 bar) would be very useful."

Specific comments: page 3 line 32 I wonder why the experiments did not go to 130 bar, at which pressure calibration gas mixtures are often distributed. The highest pressure was only 30 bar, not far above the recommended low pressure use limit of 20 bar.

The reviewer is right we should have conducted the measurements at higher pressures than 30 bar. However, the current equipment of our system would allow only pressures up to 68.9 bar (limited by the Swagelok valve). The selection of the valve was related to the condition that it does not include

any polymer parts (i.e. full metal valve). It would indeed be useful within further experiments to fill these cylinders higher than 30 bar. Our aim in this study was to establish a measurement and filling procedure and do the first characterization of this newly made cylinders. From these measurements we obtain a slope of $0.01 \mu\text{mol mol}^{-1} \text{bar}^{-1}$, which would lead to a $1.5 \mu\text{mol mol}^{-1}$ enrichment for a cylinder filled to a pressure of 150 bars and decanted to a final absolute cylinder pressure of 400 mbar. This is significantly higher than observed by Schibig et al. (2018) for instance. Therefore, we argue that at 30 bars filling pressure we are close to the maximal adsorption conditions (i.e. close to the measurable CO_2 amount fraction), as the Langmuir model says. Moreover, it is worthwhile to conduct experiments at lower pressure ranges (working pressure of analyzers) and increasing fill pressures step by step in order to understand fill pressure dependency.

For clarity we include this information in the manuscript on page 3 after line 27:

“Although the cylinders were constructed to withhold pressures up to 130 bar, the current setup would enable filling the small cylinders up to 68.9 bar which is limited by the valves (SS-4H from Swagelok). Since this study focused on the first characterization and the establishment of measurement and filling procedures of this newly made cylinders, we present experiments up to 30 bar only.”

p.4 line 12 This paragraph needs more detail, about the polishing material, what’s in the ultrasonic cleaning solution, and then later the “organic agent”, and “mild detergent”.

The commercial ultrasonic cleaning solution used in the first ultrasonic-bath is Deconex HT1201 (pH~9.4). The solution is used to remove oil, grease and residues of polishing compounds. However, we believe that either the cleaning agent or the oil residues which were still on the surface resulted in contamination during the temperature experiments. Therefore, we decided to do a second cleaning procedure. In the second ultrasonic bath a relatively neutral detergent (pH~7-8) was used since the alkaline solution (Deconex HT1201) was thought to be too aggressive. The organic agent is a chemical polishing material which was suited for aluminum surfaces.

On page 3, line 7, the following will be added:

“... a mildly alkaline commercial cleaning agent (Deconex HT1211, pH~9.4)”

On page 4, line 14, the following will be rephrased:

“Firstly, the aluminum cylinder was opened and placed in an ultrasonic-bath with a relatively neutral detergent (pH~7-8) and tap water, however the ultrasonic bath cycles at 60 °C ended with further contamination and visible stains (Fig. A1.b). To eliminate this, the two caps were polished with a chemical polishing material which was suited for aluminum surfaces...”

The stains mentioned have deposited something on the surface, but the elimination of the stains may have deposited something else later.

We agree with the reviewer that the elimination of the stains might have deposited something else on the surface of the cylinder. However, our experience was that the aluminum cylinder showed better performance after the elimination of stains without any visible changes in the surface.

p.7 section 2.3 What is the purpose of going to these low pressures, other than the small size of ice core samples? The section seems to be somewhat out of place with the rest of the experiments. Section 3.1.1 The CRDS analyzer has been used outside of its recommended range, where it cannot regulate its flow and pressure any more. There is a long description, incl. Fig. 3, of how to push a little below the factory-recommended lowest pressure. But is that relevant? Does the adsorption/desorption effect show up between the (absolute) pressures of ~1.4 and ~1.2 bar? Does any calibration gas user insist on going that low? My recommendation is to just stop at 1.4 bar, and shorten this section. It also would make the paper easier to read.

We highly appreciate our reviewer's comments on this section. However, in our opinion it is useful to include the measurements from the QCLAS analyzer, since an independent measurement device is a valuable addition for the interpretation of our current results. Moreover, presenting the lower pressure ranges is also useful for other gas applications including development of measurement systems. Although calibration gases are not used at such low limits, the aim of this study is to understand adsorption / desorption processes in its full extent including low pressures where adsorption effects should follow an exponential path.

Regarding the CRDS analyzer, our observations highlight possible systematic errors related to pressure and flow. Reporting such observations are valuable for the understanding of the measurement devices.

Section 3.1.2 I would like to thank the authors for their honest reporting, I wish more people would do that. However, also the one retained filling is a bit worrisome. Why is the response non-linear, both above and below the standard target pressure of 5 mb? Is the absorption line partially saturated?

We are confident that after our trials with the aluminum cylinder, we have established a successful procedure and used this setup for further measurements. Since these measurements were conducted after loading material blocks to the aluminum cylinder, they are not presented within this study. The runs with steel loading were reproducible, therefore, we think that presenting the one retained filling for the empty cylinder is non-problematic.

The non-linear response might indeed be related to the relatively high absorbance of the target lines (we observed this issue on two $^{12}\text{CO}_2$ lines, one of which was close to saturation which led to a significant offset in the carbon isotope ratio $^{13}\text{C}/^{12}\text{C}$). Therefore, we have selected the one which was further away from saturation, hence a saturation influence is less probable. A mismatch between the fitting model and the effective profile, crosstalk from the background or a combination of these might explain the response. It should as well be taken into consideration that the set pressure differences were large, corresponding to an order of magnitude change in the lower end (0.5 mbar).

Also, in the correction formula the fitted coefficient "c" (which corresponds to a constant offset between samples and standard) has been omitted.

The pressure correction was done relative to the cell pressure. Therefore, in Eqn. 2 (page 11, line 14) the constants (c) cancel each other.

p. 12 line 12 Note that Schibig found that even at 150 bar pressure only a relatively small fraction of available adsorption sites was occupied.

We rephrase the sentences in page 12 line 12 for clarity:

“The aluminum cylinder was in a pressure range (up to 30 bars) where most of its available sites for adsorption were unsaturated. This is in line with the observations of Schibig et al. (2018), which states that even at 150 bar pressure only a relatively small fraction of available adsorption sites was occupied. Changes between 30 and 150 bars seem to be minimal due to the shape of the adsorption isotherm.”

p.19 line 17 There is an important typo here. The “>” symbol should be changed to “<” (less than) in both cases.

We thank our reviewer for his attention. The signs are changed accordingly.

p. 19 last paragraph needs re-formulation. It now suggests that the authors have lost sight of Schibig’s observation that the Langmuir adsorption effect is only ~0.01 ppm at 75 bar, ~0.02 ppm at 45 bar, and 0.03 ppm for the 20 bar suggested cutoff. If one’s starting pressure is 30 bar, significant effects are not expected above ~4 bar, and still lower for lower starting pressures. Also the word “problematic” is an overstatement: The high reproducibility of Schibig’s results suggest that one could correct for adsorption effects. Finally, the second cleaning may have done some good, but I am not sure that is practical for the large cylinders that are mostly used.

We thank our reviewer for his insights. However, the results presented in this study have not followed the shape of the observations of Schibig et al. (2018). This difference is highly likely due to different cylinder properties used in these studies. Please see the replies to anonymous referee #2 for the discussion on K values. It would be worthwhile to investigate the adsorption using the flow-through approach. This would indicate whether the adsorption occurs already at very low pressure or not.

On page 19 line 24, we will change the word “problematic” to “not recommended”.

On page 20 after line, the following sentence will be added:

“Additionally, the reverse process of desorption will be investigated by using the flow through approach. Such experiments would be valuable to understand whether adsorption already occurs at very low pressures.”

Reply to the review of Anonymous Referee #2

The authors would like to thank anonymous referee for the valuable comments. In the following, referee's comments are given in bold and author's responses in plain text. Suggested new text is quoted in italics together with page and line numbers.

General comments: This paper investigates the trace gas stability of air stored in high pressure steel and aluminum cylinders with respect to adsorption/desorption surface processes. Experiments were designed to look at gas phase changes in CO₂, CH₄, CO and H₂O as functions of gas pressure and temperature.

The matter of trace gas stability in air standards is critical to atmospheric measurement programs. A better understanding of how surface processes affect trace gas concentrations could lead to better selection of cylinder materials and operating procedures.

This paper addresses these matters. It gives detailed descriptions of the experiments performed, which are new and informative, but the conclusions are somewhat vague. I am left with some unanswered questions.

To what extent are the results consistent with the Langmuir adsorption model?

We agree with our reviewer that this point needs further clarification. Our findings did not support the shape of the Langmuir adsorption isotherm as observed in the previous studies (Leuenberger et al. 2015, Brewer et al. 2018, Schibig et al 2018). The onset of the surface effects was not observed until sub-atmospheric pressures for the cylinders tested in this study.

In order to investigate whether the observed amount fraction changes can be explained by the Langmuir adsorption isotherm for monolayer coverage, we used a modified version of the Eqn. 5 from Leuenberger et al. (2015):

$$CO_{2,meas} - CO_{2,initial} + CO_{2,ads} = \Delta CO_2 = CO_{2,ads} \cdot \left(\frac{K \cdot (P - P_0)}{1 + K \cdot P} + (1 + K \cdot P_0) \cdot \ln \left(\frac{P_0 \cdot (1 + K \cdot P)}{P \cdot (1 + K \cdot P_0)} \right) \right)$$

Where, $CO_{2,initial} + CO_{2,ads}$ is the mean of the measured amount fractions during the first hour for each experiment. Therefore, for P close to P₀, the left side of the equation will be close to zero and it increases with lower pressures. The left term on the right hand side of the above equation is always negative and the right term always positive. Increasing K or CO_{2,ads} values increases the left term. Yet K increase is less pronounced compared to CO_{2,ads} change. K determines the curvature whereas CO_{2,ads} just stretch or compress the values.

In order to find the best possible fit, we have used R's inbuilt "optim" function with the setting Limited-memory Broyden-Fletcher-Goldfarb-Shanno (BFGS) algorithm. Upper and lower bounds were set for each unknown (CO_{2,ads} and K) and the algorithm was run to minimize the sum of squared differences between the measured amount fractions and the modelled amount fractions. For CO_{2,ads} lower and upper boundaries were set as 0.001 μmol mol⁻¹ and 15 μmol mol⁻¹. We have set the first guess values for the algorithm to the lower boundaries. In Figure 1, we show the theoretical isotherms together with our experimental data. The purple points show measurement data from the 30 bar experiments of the aluminum cylinder, and the black lines show the Langmuir monolayer fit to

the measurements with K values of 0.001 bar^{-1} and 1 bar^{-1} denoted by the solid and dashed lines, respectively. Fig 1.b shows a zoom-in to the region where the pressure in the cylinder is less than 3 bar. In order to find a better fit to the experimental data, we have further increased the upper limit of the K value up to 500 bar^{-1} (Table 1). At higher K values, the modelled curve fits better to the onset of the increasing amount fractions. The tendency of a higher K value in this study, contradicts to Schibig et al. (2018), where they have set the K value at 0.001 bar^{-1} . The difference between the estimated equilibrium constants in this study and Schibig et al. (2018) may be explained through the different surface properties (e.g. roughness or treatment of surface). Moreover, even by setting larger limits for all parameters, we did not find any K value which was able to fit the highest enrichments measured towards the end of the experiment. This might partly be related to the algorithm we have used and the limited number of data at the end of the measurements. However, the discrepancy for the highest enrichments can also be explained by another effect than desorption at low pressures. The reasonable range of K remains unclear. A more detailed analysis on model fitting is not within the scope of this experimentally focused study.

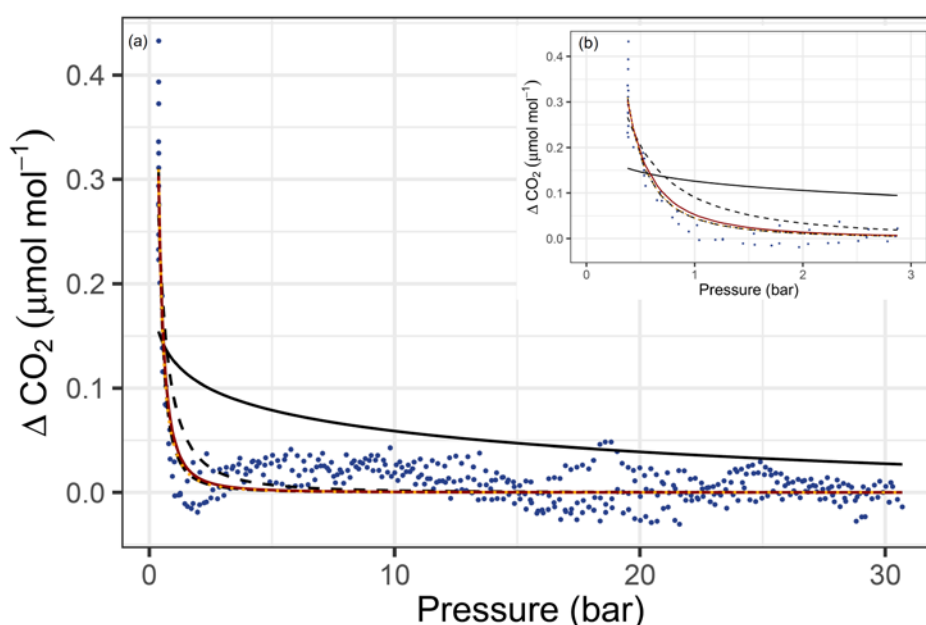


Figure 1: (a) Measured and modelled amount fractions of CO_2 for the aluminum cylinder filled to 30 bar. Purple points show measured data, black solid lines show the fit with $K=0.001 \text{ bar}^{-1}$, black dashed lines show the fit $K=1 \text{ bar}^{-1}$, dark red lines show the fit with $K=10 \text{ bar}^{-1}$, and orange dotted lines show the fit $K=100 \text{ bar}^{-1}$, and black long dashed lines show the fit $K=379 \text{ bar}^{-1}$ (b) Zoom-in to the region where the cylinder pressure is less than 3 bar.

Table 1: Model parameters for Langmuir adsorption isotherm for CRDS data

$K \text{ (bar}^{-1})$ [1]	$\text{CO}_{2, \text{ads}} \text{ (}\mu\text{mol mol}^{-1})$ [2]
0.001	0.029
1	0.015
10	0.038
100	0.301
379 [3]	1.116

[1] Upper boundary for K is increased from 0.001 bar^{-1} to 500 bar^{-1} stepwise for each solution

[2] Lower and upper boundaries for $\text{CO}_{2, \text{ads}}$ $0.001 \mu\text{mol mol}^{-1}$ and $15 \mu\text{mol mol}^{-1}$

[3] The best fit was not limited by the boundary conditions.

The following statement will be added at page 19 line 25:

“In contrast to the previous studies, the cylinders tested in this study showed enrichments only well below atmospheric pressures for the steel cylinder and the aluminum cylinder before heating. At sub atmospheric pressures, the enrichments followed a steep increase. This increase can only partly be fitted to the Langmuir adsorption isotherm if the equilibrium constant (K , the ratio between adsorption and desorption rates) are set to values higher than 1 (Supplementary material). Higher K values would correspond to higher surface coverage factors even at lower fill pressures. In comparison Schibig et al. (2018) have fixed the K value at 0.001 bar^{-1} , corresponding to lower surface coverage even at pressures of 150 bar. The reasonable range of the equilibrium constant remains unclear. The differences in the cylinder interior characteristics such as surface roughness or treatment is highly likely the explanation of the discrepancy in the K values. A further investigation on the K value and modelling approaches is not within the scope of this experimental focused study.”

Figure 1 will be added to the supplementary material together with the information on the method used for the fit.

The QCLAS measurements at sub-ambient pressures were presumably done to test the adsorption model under extreme pressure conditions. Did the experimental results support the model?

Indeed, these measurements were conducted to test the adsorption model under extreme conditions. Moreover, these measurements can also be useful for measurement systems operated at low pressure conditions. The experimental results supported the Langmuir model, however, the enrichments occurred in the region where the pressure correction function required extrapolation (page 11 line 19). Therefore, these data should be interpreted carefully. Our aim when conducting the QCLAS experiments was to find the lower limit under which CRDS measurements would be reliable. Nevertheless, we have conducted a similar analysis as presented above in order to determine model fit parameters. We add the Langmuir fit (Figure 2) to supplementary material.

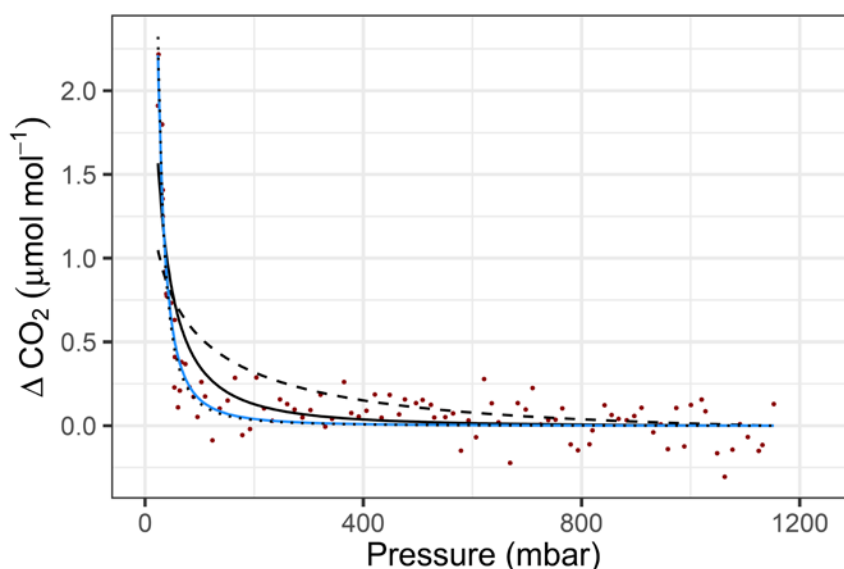


Figure 2: Measured and modelled amount fractions of CO_2 for the aluminum cylinder from the QCLAS setup. Red points show measured data, black dashed lines show the modelled fit with $K=0.001 \text{ bar}^{-1}$, black lines show the modelled fit with $K=0.01 \text{ bar}^{-1}$, blue lines show the modelled fit with $K=0.152 \text{ bar}^{-1}$ and black dotted lines show the modelled fit with $K=1 \text{ bar}^{-1}$

Table 2: Model parameters for Langmuir adsorption isotherm for QCLAS data

K (bar ⁻¹) [1]	CO _{2, ads} (μmol mol ⁻¹) [2]
0.001	0.185
0.01	0.149
0.152 [3]	0.454
1	2.387

[1] Upper boundary for K is increased from 0.001 bar⁻¹ to 1 bar⁻¹ stepwise for each solution

[2] Lower and upper boundaries for CO_{2, ads} 0.001 μmol mol⁻¹ and 15 μmol mol⁻¹

[3] The best fit was not limited by the boundary conditions.

Was the observed temperature dependency consistent with the model?

The observed temperature dependency was not consistent with the Langmuir adsorption isotherm at least above 80 °C. The temperature dependencies observed in the presented study are irreversible and not related to a physical adsorption. Within the scope of other studies (Leuenberger et al., 2015 and unpublished data), reversible temperature responses are measured until 80 °C, however these differences were an order of magnitude smaller than the presented enrichments in this study at 180 °C. Therefore, we are confident that the observed differences, above 80 °C are not related to a reversible adsorption process. The discussion on page 18 starting from line 14 explains other relevant hypotheses on the observed enrichments.

Four different gases were measured but analysis of the results focuses on CO₂. This may be because CO₂ showed the strongest signals, but the authors should comment on why this is the case, and provide some more discussion of what the results say about the other gases. For example, do the gases differ in their sensitivity to adsorption on account of their molecular properties? Can this explain the different pressure and temperature dependencies observed for the different gases?

We agree with our reviewer that more information on other species is necessary. The reason that our study concentrate on CO₂ is indeed related to the strong amount fraction response of CO₂.

The following paragraph will be added at page 19 after line 31:

“This study also showed that the measured gases CO, CO₂, CH₄ and H₂O had different sensitivities with respect to surface processes. We have observed surface effects for CO₂ and H₂O. Observed effects of H₂O during the pressure experiments were an order of magnitude larger than CO₂ (not shown here). One of the explanations that CO₂ and H₂O are more prone to surface effects might be due to their high boiling points. CO₂ sublimates at -78.5 °C, and the boiling point of H₂O is 100 °C. Whereas for CH₄ and CO, boiling points are -161 °C and -191.5 °C, respectively. Since CO is a reactive compound, it might be argued that it would be more prone to surface effects. However, our results have shown that CO in atmospheric air was not affected by surface interactions at short time scales (in the order of days). This is highly likely related to the competitive adsorption between species. The ratio between the amount fraction of CO and CO₂ would be 1 to several hundreds. In order to understand competitive adsorption to its full extent, experiments focusing on a range of amount fractions would be useful. Moreover, when discussing adsorption properties, polarity is also an

important criterion. Therefore, the non-polar structure of CH₄ makes it less prone to adsorption, whereas the polar geometry of H₂O enables it to be more adsorptive.”

What conclusions can be drawn for how air standards should be prepared and used?

The air standards should not be stored at high temperatures. However, high temperatures might be useful for pre-treatments of cylinders. Aluminum cylinders are well suited to store greenhouse gases such as CO, CO₂ and CH₄, whereas usage of stainless steel cylinders are more suited for standards of halogenated compounds.

I think the paper could be suitable for publication in AMT if these questions are addressed.

Specific comments:

It is unclear in some parts of the text if quoted gas pressures are absolute or relative to ambient atmospheric pressure. There is potential for more confusion when referring to cylinder and cell pressures.

We agree with our reviewer this point need clarification. Cell pressures are consistently reported as absolute pressures, whereas cylinder fill pressures for CRDS measurements are consistently reported relative to the ambient pressure. We make the following additions to the manuscript in order to prevent confusion:

On page 1, line 9:

“This extensive dataset revealed that for absolute pressures down to 150 mbar the enhancement in the amount fraction of CO₂ relative to its initial value (at 1200 mbar absolute) ...”

In Table 1 on page 6,

“[bar relative to atm]”

On page 7, line 16:

“Therefore, we filled the aluminum cylinder to 1200 mbar (absolute)”

On page 10, caption of Figure 5:

“Reported pressure data show absolute pressure values.”

On Page 11, line 17:

“At the point where the cell pressure started to fall below the target pressure (150 mbar absolute-Fig. 5c) ...”

On page 12, caption of Figure 6:

“x-axes show the absolute pressure values in the sample cylinder.”

On page 19, line 5:

“The independent QCLAS measurements on the aluminum cylinder has not shown any effect down to absolute pressures as low as 150 mbar.”

On page 20, line 11:

“The results showed that for absolute pressures above 150 mbar... “

Page 8, line 4 – It should be noted here that CH₄ decreased while the other three gases increased in concentration. What does this say about the favored explanation of outgassing?

Our reviewer points out an interesting point, however, the underlying mechanism of the instrument related effects are unclear. The decrease in CH₄ might partly be related to a dilution caused by the increase of other compounds in the cavity.

Page 12, line 2 – It is claimed that CO and CH₄ dependency on pressure was not significant, but in Figure 6 for CH₄ at least, the “Steel before heating” and “Aluminum after heating” plots show elevated CH₄ at low pressures. Is this an analytical artefact or a real bias? If real, it requires some comment. The authors should also comment on why there is a clear effect for CO₂ and H₂O but not for CO and CH₄.

We thank the reviewer for pointing this out. We relate these changes to an analytical artefact likely related to a drift in CH₄ measurements and the cavity pressure instabilities which occurred towards the end of the experiments. Since the onset of this increase is not the same for the conducted experiments and the observed differences are not consistent through the replicates, we do not relate these effects to adsorption / desorption processes. Fig. 7c clearly shows the differences among the replicates of steel cylinder, and the aluminum after heating experiments.

Please see the text above for explanation of the adsorptive properties of all measured species.

Page 15, Section 3.3.2 – It appears that all four gases are correlated in their response to temperature changes. If so this should be made clear. Is there a reason why the figures and the table consider only correlations between the pairs CO₂ – CH₄ and CO – H₂O?

We agree with the reviewer that this point needs clarification. Indeed, all pairs are correlated, for easier visibility only two pairs at a time was shown. The species were paired by highest coefficient of determinations.

The reason behind such correlations might be chemical reactions following fixed ratios of production, however it is highly questionable if it is feasible to produce methane under 180 °C and slightly over 10 bar. This is already explained on page 18 lines 14-18.

The readability of the paper is fairly good, but could be improved in places with a little attention from a proficient English speaker. Maybe the editor could help with this. Some specific suggestions are included below.

We thank our reviewer for his attention, the technical corrections noted below are changed at the respective places.

Technical comments:

Page 1, line 9 – replace “until pressures as low as 150 mbar” with “for pressures down to 150 mbar” – text modified accordingly

Page 1, line 17 – reword to “measurements of CO₂ were made at Mauna Loa, Hawaii in the late 1950s...” – text modified accordingly

Page 1, line 19 – “with an increasing number” - corrected

Page 1, line 21 – Global Atmosphere Watch - corrected

Page 2, line 13 – has received attention - corrected

Page 2, line 18 – amount fractions - corrected

Page 2, line 25 – gas cylinder usage - corrected

Page 3, line 3 – reword to “enables placement of test materials...” - corrected

Page 3, line 31 – interpret - corrected

Page 4, lines 1-2 – Provide some more detail about the flow rate used and the length of time required to obtain reliable measurements. Was there significant change in cylinder pressure?

The flow rate during the pressure experiments is shown in Fig. 4a. The flow rate into the cell of the CRDS analyzer is between 15 mL min⁻¹ and to 220 mL min⁻¹, regulated by the outlet valve as explained in Sect. 3.1.1. Regarding the time required, the measurement setup has 1/4" tubing which is 30 cm long. Prior to the experiment, the tubing and the pressure regulator were flushed 3 times. For the analysis the first 10 minutes of data was not taken into consideration. 10 minutes of measurements with 220 mL min⁻¹ would correspond to a 0.4 bar decrease in the pressure of the small cylinder. Since the observed effects in the cylinders does not start until pressures less than atmospheric pressures, the change is not significant for the presented experiments.

For clarity we include this information also in Page 4 line 3:

“There was no flow regulation after the pressure regulator prior to the analyzer inlet. At the beginning of the experiment the flow rate was 220 mL min⁻¹ (STP) and towards the end of the experiment it was 15 mL min⁻¹(STP). More information on flow rate is included in Sect. 3.1.1. The measurement setup had 1/4" tubing of 30 cm. long. Prior to the experiment, the tubing and the pressure regulator were flushed 3 times. For the analysis the first 10 minutes of data was not taken into consideration.”

Investigation of adsorption/desorption behavior of small volume cylinders and its relevance for atmospheric trace gas analysis

Ece Satar^{1,2}, Peter Nyfeler^{1,2}, Bernhard Bereiter^{1,2,3}, Céline Pascale⁴, Bernhard Niederhauser⁴, and Markus Leuenberger^{1,2}

¹Climate and Environmental Physics, Physics Institute, University of Bern, Bern, Switzerland

²Oeschger Centre for Climate Change Research, University of Bern, Bern, Switzerland

³Empa, Laboratory for Air Pollution / Environmental Technology, Dübendorf, Switzerland

⁴Federal Institute of Metrology METAS, Bern, Switzerland

Correspondence: satar@climate.unibe.ch

Abstract. Atmospheric trace gas measurements of greenhouse gases are critical in their precision and accuracy. In the past 5 years, atmospheric measurement and gas metrology communities have turned their attention to possible surface effects due to pressure and temperature variations during a standard cylinder's lifetime. This study concentrates on this issue by introducing newly built small volume aluminum and steel cylinders which enable the investigation of trace gases and their affinity for adsorption/desorption on various surfaces over a set of temperature and pressure ranges. The presented experiments are designed to test the filling pressure dependencies up to 30 bar, and temperature dependencies from $-10\text{ }^{\circ}\text{C}$ up to $180\text{ }^{\circ}\text{C}$ for these prototype cylinders. We present measurements of CO_2 , CH_4 , CO and H_2O using a cavity ring down spectroscopy analyzer under these conditions. Moreover, we investigated CO_2 amount fractions using a novel quantum cascade laser spectrometer system enabling measurements at pressures as low as 5 mbar. This extensive dataset revealed that ~~until pressures as low~~ as for absolute pressures down to 150 mbar the enhancement in the amount fraction of CO_2 relative to its initial value (at 1200 mbar absolute) is limited to $0.12\text{ }\mu\text{mol mol}^{-1}$ for the prototype aluminum cylinder. Up to $80\text{ }^{\circ}\text{C}$, the aluminum cylinder showed superior results and less response to varying temperature compared to the steel cylinder. For CO_2 , these changes were insignificant at $80\text{ }^{\circ}\text{C}$ for the aluminum cylinder, whereas a $0.11\text{ }\mu\text{mol mol}^{-1}$ enhancement for the steel cylinder was observed. High temperature experiments showed that for both cylinders irreversible temperature effects occur especially above $130\text{ }^{\circ}\text{C}$.

1 Introduction

Atmospheric measurements play a crucial role in understanding the global carbon cycle and its response to anthropogenic perturbation. The first atmospheric measurements of CO_2 were ~~done in~~ made at Hawaii in Mauna Loa in the late 1950s (Pales and Keeling, 1965). Ever since, the number of stations for atmospheric observations has increased continuously. Most of these measurements are conducted in remote areas, and with an increasing number of stations it is more challenging to ensure the comparability of the measurements. The coordination of the greenhouse gas measurement network is achieved by the World Meteorological Organization (WMO) through its Global ~~Atmospheric~~ Atmosphere Watch Programme (GAW). WMO also makes recommendations on the compatibility targets for the measurement stations within its network. For CO_2 , these

targets correspond to $0.1 \mu\text{mol mol}^{-1}$ for the northern hemisphere, and $0.05 \mu\text{mol mol}^{-1}$ for the southern hemisphere (WMO, 2018). These ambitious targets allow the interpretations of fluxes on global and continental scales, and to better distinguish the underlying processes (Rödenbeck et al., 2006; Masarie et al., 2011).

In order to ensure quality observations, the measurement systems are calibrated regularly with known standards. In addition to careful and regular calibrations, it is important to be able to account for the instabilities which might affect the measured amount fractions of trace gases. More than a decade ago, Langenfelds et al. (2005) and Keeling et al. (2007) have reported deviations of O_2/N_2 and CO_2 in standard cylinders. The former study has suggested that diffusive fractionation is the main process, however for CO_2 diffusive fractionation alone was not sufficient to explain the observed enrichment. The latter study reported a downwards drift in their aluminum cylinders with respect to steel cylinders. Keeling et al. (2007) explained this difference by conditioning wall reactions. These studies also mention leakage, regulator effects, and thermal and gravimetric fractionation as responsible processes for instabilities.

With the advances in analytical techniques and improvements in measurement uncertainties, more stringent targets of better comparability became possible. The discussion on surface effects has ~~got~~received attention in the last five years within both atmospheric measurement and gas metrology communities. For CO_2 , the studies from Leuenberger et al. (2015) and Miller et al. (2015) interpreted their findings in favor of adsorption and desorption processes. Leuenberger et al. (2015) emptied the cylinders and observed enrichments in the amount fractions of CO_2 due to pressure loss, whereas Miller et al. (2015) filled the cylinders and calculated mother to daughter ratios and reported losses to gas wetted surfaces. Moreover, Leuenberger et al. (2015) used Langmuir (1918) monolayer adsorption isotherm to explain the observed enrichment in CO_2 ~~ament~~amount fractions. These studies were followed by another pair of studies from both communities (Brewer et al., 2018; Schibig et al., 2018). These experiments were designed to include also cylinders with surface passivation and different water vapor content. The results of these studies confirmed that adsorption/desorption processes is at play, but also Rayleigh fractionation during high flow experiments plays a role (Schibig et al., 2018).

This study contributes to currently existing literature by presenting data on below ambient pressures and high temperatures separately. The experiments are done using two newly built small volume aluminum and steel cylinders. This paper focuses on several issues related to gas ~~eylinders~~cylinder usage: (i) pressure dependency of surface processes with respect to filling pressure, (ii) pressure relation of adsorption/desorption for very low pressure ranges, and (iii) possible effects of heating on cylinders.

2 Data and Methods

2.1 Production and filling history of the small cylinders

In order to understand adsorption/desorption effects to its full extent, we scaled down the problem. For this purpose, high pressure (up to 130 bar) and small volume (5 L) cylinders of aluminum and steel were designed. The aluminum cylinder is made of the aluminum alloy AlMg1SiCu (EN AW-6061), and the steel cylinder is made of hardened and tempered steel (1.7218

/ 25CrMo4, EN 10273). The cylinder compositions are specifically chosen such that they correspond to steel and aluminum materials commonly in use for high pressure cylinders in the atmospheric measurement community.

The 5 L cylinders are formed from raw materials without welding at the workshop of the University of Bern. Each cylinder consists of three pieces (Fig. A1a): a body part in the middle with two caps on the sides. These pieces are joined by twelve necked-down bolts on each side, and Inconel X750 seals with silver coating are placed in the caps. This setup enables ~~to place~~ placement of test materials into these chambers to investigate their surface effects.

After their production at the workshop of the University of Bern, the cylinders were sent to the external firm that designed them for pressure testing and certification for usage at high pressures. Then, the cylinders underwent a cleaning procedure consisting of ultrasonic bath with a diluted solution of a mildly alkaline commercial cleaning agent (Deconex HT1201, pH~9.4), and oven drying (Table 1a).

Each cylinder is equipped with four full-metal valves (SS-4H from Swagelok). All tubings (1/4") and connections are made of stainless steel, while the tubings are also electropolished. At the outlet, the cylinders are equipped with a dual stage pressure regulator made of stainless steel with a polychlorotrifluoroethylene (PCTFE) seat (64-3441KA412 from Tescom). Pressure transducers are used at low (PTU-S-AC6-31AC from Swagelok), and high (PTU-S-AC160-31AC from Swagelok) pressure sides of the pressure regulators. Temperature sensors spanning a range from ~~-35~~-35 °C to +100 °C (AF25.PT100 from Thermokon) are placed on the outer cylinder surfaces and one is placed on a pressure regulator. All measured temperature and pressure data were read and logged by a signal converter (midi logger GL820 from Graphtec). For experiments exceeding 100 °C another digital thermometer (Greisinger GMH 3250) was used.

The filling history of the small cylinders is the following: They were filled with N₂ (Alphagaz 2 N₂) up to 2 bar (relative to ambient pressure) for background measurements (data not presented here). According to its specifications, Alphagaz 2 N₂ contains very low amount fractions of CO (< 0.1 μmol mol⁻¹), CO₂ (< 0.1 μmol mol⁻¹), CH₄ (< 0.1 μmol mol⁻¹) and H₂O (< 0.5 μmol mol⁻¹). The rest of the fillings were done using high pressure 50 ~~H~~L aluminum cylinders with compressed air. These aluminum cylinders (LUX3588, LUX3575, and LUX3586) are referred to as mother cylinders from here on. A scheme of the measurement setup is given in Fig. 1a. The fillings which did not exceed 6 bar were conducted directly through the pressure regulator same type as above (64-3441KA412 from Tescom), and the fillings exceeding 6 bar were done by expansion. In this case, the mother cylinder was directly connected to a small expansion volume (0.5 L) of stainless steel (316L-HDF4-500 from Swagelok). The desired pressure in the small cylinder was achieved by repeating the expansion step several times. Bracketing each sample measurement, another aluminum cylinder of comparable material and equipment to the mother cylinder was measured to check the stability of the measurement device (LUX3579).

Although the cylinders were constructed to withstand pressures up to 130 bar, the current setup would enable filling the small cylinders up to 68.9 bar which is limited by the valves (SS-4H from Swagelok). Since this study focused on the first characterization and the establishment of measurement and filling procedures of this newly made cylinders, we present experiments up to 30 bar only.

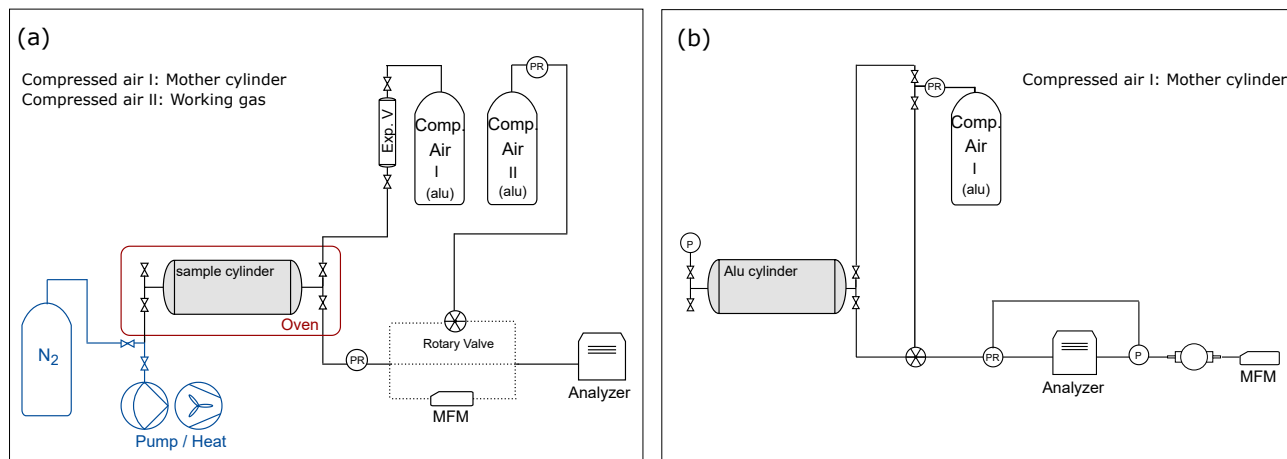


Figure 1. Measurement schemes: **(a)** CRDS analyzer. The sample cylinder is filled by expansion from the mother cylinder, and placed in the climate cabinet (red box) for the temperature experiments. Dotted lines show the three different pathways between the outlet of the cylinder and the inlet of the analyzer. During temperature experiments, sample gas flows through the rotary valve, during several experiments (Table 1h) sample gas flows through mass flow meter (MFM) to monitor flow. For all remaining experiments, the sample gas is directed to the analyzer with electropolished stainless steel tubing. The equipment used for the cleaning procedure applied in between experiments in Table 1e is shown in blue. **(b)** QCLAS system. The sample cylinder is filled through the pressure regulator. The inflow to the analyzer is switched between the mother and sample cylinder through the rotary valve. The loop around the analyzer shows the pressure regulation (See Sect. 2.3 for a detailed description). After the turbomolecular pump a MFM is placed to monitor outflow.

2.2 Experiments with CRDS analyzer

Both temperature and pressure experiments were conducted using these newly built cylinders. An overview of all presented experiments and procedures are given in Table 1. The presented experiments cover in total two years, and the chronology of the experiments and procedures are essential to [interpret](#) the results.

- 5 In order to investigate pressure dependency, the aluminum cylinder was filled in five pressure levels (1.5, 6, 8, 20 and 30 bar) and the steel cylinder was filled in four pressure levels (6, 8, 20 and 30 bar) (Table 1b). Each measurement series had at least three replicates. For pressure experiments, the small cylinders were filled, and an hour was given for equilibration. Then, the cylinder was measured continuously with a Picarro Cavity Ring Down Spectroscopy (CRDS) G2401 analyzer, allowing measurements of CO₂, CO, CH₄ and H₂O. In between the experiments, the cylinders were only pumped through the analyzers
- 10 external pump, and the next filling was done without flushing with another gas. [There was no flow regulation after the pressure regulator prior to the analyzer inlet. At the beginning of the experiment the flow rate was 220 mL min⁻¹ \(STP\) and towards the end of the experiment it was 15 mL min⁻¹ \(STP\). More information on flow rate is included in Sect. 3.1.1. The measurement setup had 1/4" tubing of 30 cm long. Prior to the experiment, the tubing and the pressure regulator were flushed 3 times. For the analysis the first 10 minutes of data was not taken into consideration.](#)

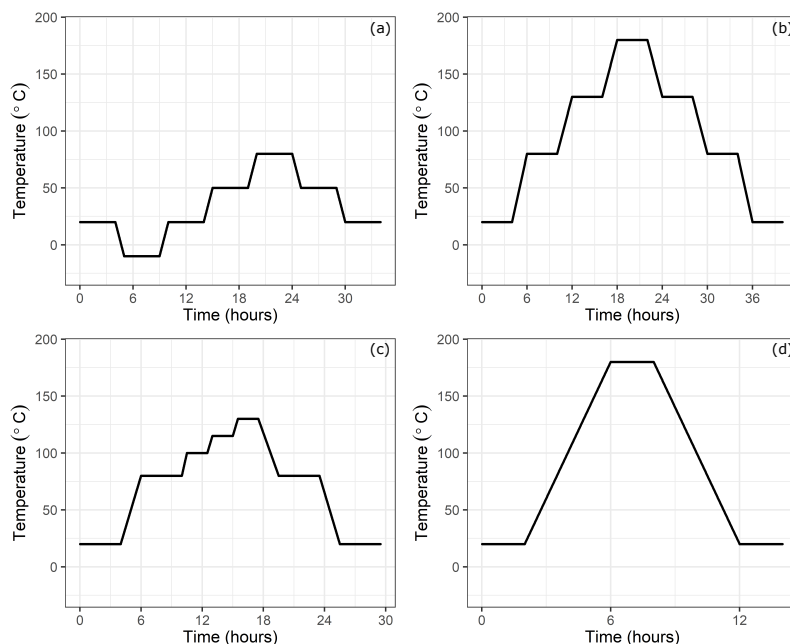


Figure 2. Temperature setting at the climate cabinet: (a) low temperature experiments, (b) high temperature experiments, (c) experiments until 130 °C and (d) high temperature experiments for only 180 °C.

In order to investigate the temperature dependency, the small cylinders were placed into a climate cabinet (ACS Challenge 600) at the Swiss Federal Institute of Metrology (METAS). The temperature of the cabinet was set at temperatures from – 10 °C to 180 °C (Table 1c). For low temperature experiments, the temperature was set at –10 °C, 20 °C, 50 °C and 80 °C, with 30 °C increments, heated or cooled within an hour (Fig. 2a). Whereas for high temperature experiments, temperature was set at 20 °C, 80 °C, 130 °C and 180 °C, and heated or cooled within two hours (Fig. 2b). The set temperature was kept constant for four hours at each level, of which during the last 35 minutes the sample cylinder was measured. These measurements were bracketed by working gas measurements (LUX3579) which did not experience any temperature changes. A multiport valve (EMT2CSD6MWE from VICI AG) was used to switch between the small cylinders and the working gas.

Moreover, we applied a further cleaning procedure during the course of the temperature experiment set (Table 1d). This corresponded to heating and pumping cycles of several hours at 180 °C for the steel cylinder; and opening, ultrasonic cleaning, and polishing for the aluminum cylinder. Firstly, the aluminum cylinder was opened and placed in an ultrasonic-bath with a mild-detergent-relatively neutral detergent (pH~7-8) and tap water, however the ultrasonic bath cycles at 60 °C ended with further contamination and visible stains (Fig. A1b). To eliminate this, the two caps were polished with an-organic-agent-a-chemical polishing material which was suited for aluminum surfaces, and the cylinder underwent a further cycle of ultrasonic bath with a-mild-detergent-detergent (pH~7-8) and tap water, followed by three cycles of cleaning with tap water and a final round with reverse osmosis water.

After the second cleaning procedure, to investigate the high temperature effects in more detail, we did several fillings with synthetic air and N₂ (Table 1e) with fewer step changes at various temperatures (Fig. 2d).

Due to the fact that heating of cylinders led to contamination, we established a cleaning procedure consisting of three pump-heat cycles of 30 minutes each in between the temperature experiments presented in Table 1e. During each cycle, cylinders
5 were filled with 2 bar N₂, and while pumping, the cylinder was heated by a heat gun, where its surface temperature did not exceed 60 °C. The cylinder was pumped using a dry piston vacuum pump (EcoDry M15 from Leybold) until 0.05 mbar.

For better comparison of pressure behavior after temperature experiments and cleaning, we included data from a filling pressure of 14 bar (Table 1f). These experiments were conducted within another study related to these cylinders (Satar et al., 2019). And lastly, we did several fillings of 3.5 bar (Table 1h). For these last measurements a mass flow meter (Series 358 from
10 Analyt - MTC) was placed at the inlet or at the outlet of the analyzer in order to monitor flow.

~~Temperature setting at the climate cabinet: (a) low temperature experiments, (b) high temperature experiments, (c) experiments until 130 °C and (d) high temperature experiments for only 180 °C.~~

In order to compare different datasets, measured amount fractions were subtracted from the mean of the first hour of measurements for each run. Then, 5-minute means of these differences were calculated in order to eliminate instrumental noise. All
15 reported values in this study from the CRDS analyzer are differences of amount-of-substance fractions and denoted by ΔCO_2 , ΔCO , ΔCH_4 and $\Delta\text{H}_2\text{O}$.

2.3 Experiments with dual Quantum Cascade Lasers Absorption Spectrometer (QCLAS)

In order to understand the surface processes to its full extent, the aluminum cylinder was tested at pressures as low as 5 mbar using a novel analyzer (Table 1g). These measurements were conducted at the Swiss Federal Laboratories for Material
20 Science and Technology (Empa). The analytical approach is based on direct absorption spectroscopy using Quantum Cascade Lasers (QCLs) (Nelson et al., 2008; McManus et al., 2011). The spectrometer used in this study is built within the deepSLice project for measuring air samples of very small volumes such as 1-2 mL STP extracted from ice-cores, and is under further development. The analyzer enables simultaneous measurements of CO₂, CH₄ and N₂O amount fractions and the isotopic signature of CO₂. In order to cover all four target species in mid-infrared spectral range, the system is equipped with two
25 quantum cascade lasers emitting at 4.3 and 7.7 μm , respectively. Furthermore, the analyzer is optimized for low gas pressures (~ 5 mbar) in its cell to cope with the small amount of sample available from ice samples.

Figure 1b shows the measurement setup for these experiments. We aimed to cover the range from atmospheric to sub-atmospheric pressures until the cell pressure of 5 mbar. Therefore, we filled the aluminum cylinder to ~~200 mbar (relative to ambient pressure)~~ 1200 mbar (absolute) using the same type of pressure regulator as in Sect. 2.1. The cylinder was evacuated
30 using a turbo pump at the end of the line. In order to eliminate instrumental drift, the mother cylinder was measured for five minutes every 15 minutes bracketing the measurements from the sample cylinder. The multiport valve (EUTA-SD6MWE from VICI) allowed switching between the mother cylinder and the small aluminum cylinder. After the rotary valve, the gas entering the measurement cell was controlled by a pressure controlling loop using a proportional valve (EV-P-10-0925 from Clippard) coupled with a controller (JumodTron316), and a pressure transmitter (PAA-35X Series from Keller) after the cell and before

Table 1. An overview of experiments and procedures included in this study in chronological order

a. First cleaning – February 2017				
Aluminum – Steel	Ultrasonic bath and oven dried			
Cylinder	Experiment	2*Pressure <u>bar</u> Pressure <u>[bar relative to atm]</u>	Number of replicates	Mother cylinder
b. Pressure experiments with CRDS – February 2017 – June 2017				
Aluminum	Pressure	1.4 ... 1.5	4	LUX3588
Aluminum	Pressure	5.7 ... 5.8	4	LUX3588
Steel	Pressure	5.7 ... 6.0	4	LUX3588
Steel	Pressure	7.3 - 7.3 - 7.5	3	LUX3588
Steel	Pressure	18.6 ... 20.8	4	LUX3588
Steel	Pressure	24.3 - 25.4 - 26.4	3	LUX3588
Aluminum	Pressure	7.5 - 7.7 - 8.0	3	LUX3588
Aluminum	Pressure	16.9 - 17.8 - 18.6	3	LUX3588
Aluminum	Pressure	28.3 - 29.4 - 29.8	3	LUX3588
c. Low and high temperature experiments with CRDS – June 2017 – August 2017				
Aluminum	Low T: -10 °C - 80 °C	26	1	LUX3588
Aluminum	High T: 20 °C - 180 °C	23.8	1	LUX3588
Steel	Low T: -10 °C - 80 °C	23.3	1	LUX3588
Steel	High T: 20 °C - 180 °C	21.9 - 20.5 - 19.3	3	LUX3588
Steel	Up to 130 °C	18.1	1	LUX3588
d. Second cleaning – August 2017				
Aluminum	Opened, ultrasonic bath, and polished			
Steel	Pump-heat cycles of several hours at 180 °C			
e. High temperature experiments with CRDS after cleaning – September 2017				
Aluminum*	After cleaning: 20 °C - 180 °C	4.81	1	LUX3588
Steel	After cleaning: 20 °C - 180 °C	4.4- 4.5 - 4.6	3	LUX3588
Aluminum*	High T: 20 °C - 180 °C **	4.5 - 4.6	2	Synthetic air
Steel*	High T: 20 °C - 180 °C	4.6	1	Synthetic air
Aluminum*	High T: 20 °C - 80 °C - 180 °C	5.0	1	N ₂
Steel*	High T: 20 °C - 80 °C - 180 °C	5.1	1	N ₂
f. Pressure experiments with CRDS – September 2018				
Aluminum	Pressure	13.9 – 13.9	2	LUX3575
g. Experiments with QCLAS – October 2018				
Aluminum	Pressure	0.2	6	LUX3575
h. Pressure experiments with CRDS – November 2018 – January 2019				
Aluminum	Pressure	3.3 ... 3.7	10	LUX3575
Aluminum with MFM***	Pressure	3.4 - 3.8- 4.2	3	LUX3575

*Fill-pump-heat cycles with N₂ prior to filling

**One run with High T: 20 °C - 80 °C - 180 °C

***MFM: Mass flow meter

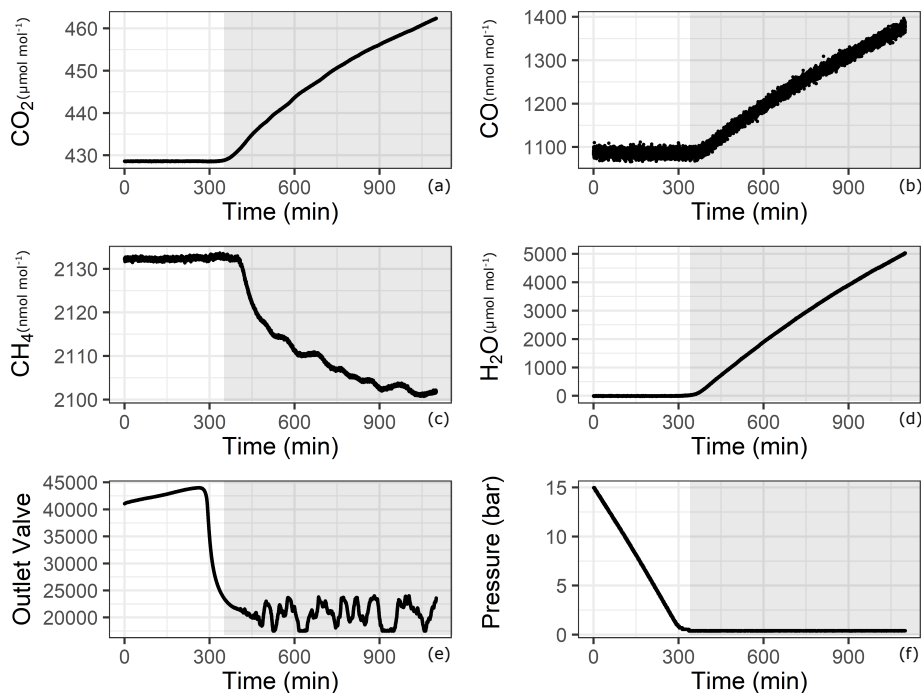


Figure 3. Analyzer response with respect to time for (a) CO₂, (b) CO, (c) CH₄, (d) H₂O, (e) Outlet Valve and (f) Pressure in the cylinder. Shaded areas correspond to depletion of sample flow.

the pump. This control loop enabled measurements of the sample cylinder without a pressure regulator after the outlet of the cylinder, and provided constant flow conditions at a set cell pressure of 5 mbar. The mother cylinder underwent the same pressure control loop, however for the mother cylinder a pressure regulator was used to preset the supplied pressure close to atmospheric pressure. After the turbo pump, a mass flow meter (Series 358 from Analyt - MTC) was placed in order to monitor the flow out of the analyzer.

3 Results

3.1 Data analysis

3.1.1 Pressure experiments with CRDS

Since adsorption/desorption processes are pressure dependent, we aimed to cover the widest pressure range using a CRDS analyzer. However, this is not trivial since our measurements started from pressures as high as 30 bar, which was reduced by a pressure regulator to a pressure of 30 mbar (relative to ambient pressure) before the analyzer inlet. During the course of evacuation, the high pressure side of the regulator approached atmospheric pressure, and towards the end of the experiment, the

regulator had no pressure difference to regulate. Under conditions of very low to no-flow, the CRDS analyzer started to show an effect of increasing amount fractions of CO and CO₂, and H₂O. This effect is illustrated in Fig. 3 for one of the experiments with 14 bar in the aluminum cylinder (Table 1f). The increase is proven not to be due to a leak in the measurement line or in the analyzer, since the measured amount fraction of CO (Fig. 3b) showed an increasing trend even when the initial amount fraction in the cylinder was 10 times higher than for laboratory air. Some possible reasons for this effect might be thermal diffusion or outgassing of parts in CRDS analyzer close to the cavity. Indeed, there exists a temperature gradient between the cavity (45 °C) and the cylinder (room temperature around 25 °C). However, it is unlikely that thermal diffusion is responsible for this enhancement, since both molecules with lower molecular weights such as H₂O and CO, and with higher molecular weights such as CO₂ accumulated at the high temperature side. Moreover, the analyzer showed the same behavior when the cylinder was disconnected. Outgassing of materials close to the cavity seems to be the most likely reason for this increase, and thus it was hard to locate the exact responsible component. Even though this increase remains unclear, it is obvious that this effect is neither related to the cylinder, nor to the pressure regulator, but is originating from the analyzer. Therefore, a cut-off point for the datasets is needed according to valid criteria. A possible criterion to set a cut-off point is using the CO measurements, and set the end point when CO amount fraction starts to increase. Another option would be setting a minimum inflow to the analyzer limiting the residence time in the cavity. Lastly, applying a method using the correlation between an internal variable of the analyzer (outlet valve) and measured variables (low pressure reading of the pressure regulator) would lead to a reasonable cut-off point. All methods have their advantages and disadvantages, i.e., criteria based on CO measurements or pressure reading suffer from the quality of the measurement and its lower precision. In this section we focus on the flow criteria. Detailed information on the remaining two methods and their application are provided in the supplementary material.

The presented method aims to provide an end point which ensures sufficient flow through the analyzer. It is important to note that according to the datasheet of the G2401 CRDS analyzer, the inlet pressure is suited to be as low as 400 mbar. A possible approach would be using the pressure at the inlet of the analyzer from the reading of the pressure transducer at the low pressure side of the pressure regulator. Since these pressure values are measured relative to atmospheric pressure, we preferred the alternative of linking our measurements to the output of an internal variable of the analyzer called the “outlet valve”. This proportional valve controls the gas amount, respectively the pressure in the cavity. For the Picarro CRDS G2401 used in these experiments, the maximum value of the outlet valve is 65000 corresponding to fully open, and the minimum value is 17500 corresponding to fully closed. In case of high gas flow, the outlet valve opens and more gas is pumped out of the cavity, whereas when the inflow to the instrument decreases, the outlet valve closes in order to keep the gas in the cavity and avoid pressure decrease. This regulation is achieved in such a way that the cell pressure is controlled to 140 ± 0.15 Torr (186.65 ± 0.20 mbar).

The analyzer response does not correspond to reasonable values when the outlet valve values are lower than around 21500. This lower limit of the outlet valve can be validated for each measurement run individually by the first method we applied using the CO amount fraction increase (Supplementary material). Since our measurements were already in a region out of the specification range of the analyzer, we aimed to validate the cut-off point in a more conservative manner than relying on the CO measurements. As an alternative, we chose to monitor the flow rate into / out of the analyzer. In order to achieve this, we

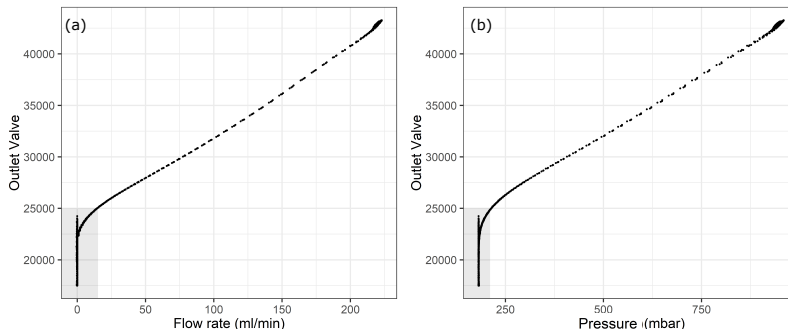


Figure 4. Flow parameters into the analyzer with respect to the internal parameter outlet valve (a) Flow rate, and (b) Pressure at the outlet of the pressure regulator. Shaded areas correspond to depletion of sample flow.

placed a mass flow meter (MFM) either just before the analyzer inlet or after the pump at the outlet of the analyzer (Table 1h). In Fig. 4, the outlet valve value is shown against the flow and the pressure at the inlet of the instrument. Here, shaded areas show a possible cut-off point for the experiments at 25000 for the outlet valve value with a non-zero inflow to the instrument. Since our aim was to find the minimum inflow to the instrument, and corresponding residence time, we estimated the amount of sample air in the cavity of the analyzer as 5.6 mL STP, by inserting 140 Torr, 45 °C, and 35 mL for cavity pressure, temperature and volume into the ideal gas equation. At STP conditions and 25000 outlet valve value, flow rate into the analyzer was 15 mL min⁻¹, which accounts to flushing of the cavity less than every 30 seconds. Since we reported our results in 5-minute means, we allowed at least 10 times the residence time of the cavity to flush probable outgassing effects. In terms of pressure this cut-off point corresponded to 214 mbar, which was significantly lower than 400 mbar. In order to validate the selected cut-off point, we used an independent measurement system (Sect. 2.3), the results at low pressures are presented in the following section.

3.1.2 Pressure experiments at low pressures using QCLAS

We have done six fillings for the empty aluminum cylinder, and three fillings with steel loading inside the aluminum cylinder (data not presented in this study). From these six fillings, only one has resulted in reasonable data. Other experiment runs have suffered from various problems such as data acquisition failure, and setting the pressure regulator of the mother cylinder to sub-atmospheric pressures.

Even though the system accounts for pressure broadening effects in the spectral analysis, there remains a pressure dependence if the cell pressure during a sample measurement is not the same as during a standard (mother cylinder) measurement. Since the pressure in the sample cylinder decreased over the experiment but the mother cylinder provided constant pressure, the cell pressure of the samples started to fall below the targeted 5 mbar cell pressure (at about 150 mbar absolute pressure in the sample cylinder - Fig. 5d). In order to correct for this effect, the following experiment was performed: Starting from 10 mbar until 0.5 mbar with 0.5 mbar steps and back again, the cell target pressure was changed every seven minutes, while in

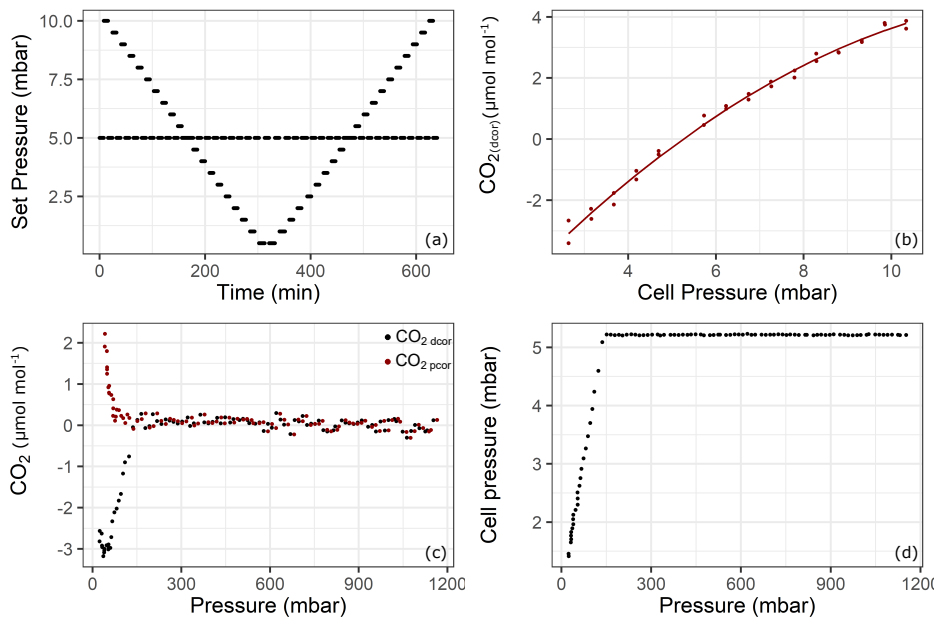


Figure 5. Results of the pressure experiment using QCLAS. The top panel shows the results from the cell pressure experiment: (a) Set pressure, (b) CO₂ response to changing cell pressure. The lower panel shows the experiment using the sample aluminum cylinder: (c) drift corrected CO₂ amount fractions (black) and pressure corrected CO₂ amount fractions (red), and (d) cell pressure changes during the emptying of cylinder from 1200 mbar to 15 mbar. [Reported pressure data show absolute pressure values.](#)

between each of these steps, the pressure was set to the standard target pressure of 5 mbar (Fig. 5a). The measurements were first corrected for drift by subtracting the standard measurement at 5 mbar from the “sample” measurements at each pressure. Then, the following second-order polynomial was fitted to the data (Fig. 5b) to derive a cell pressure correction function:

$$x_{dcor} = a \cdot p_{set}^2 + b \cdot p_{set} + c \quad (1)$$

- 5 where, x_{dcor} is the drift corrected amount fraction of substance, p_{set} is the set pressure for the measurement cell, and a , b and c are the coefficients of the fit. The coefficient of determination (r^2) of the fit is 0.99. Finally, drift corrected measurement data from the fillings were corrected for pressure according to:

$$x_{pcor} = x_{dcor} - (p - p_{std}) \cdot b - (p^2 - p_{std}^2) \cdot a \quad (2)$$

where, p is the cell pressure during the measurement and p_{std} is the cell pressure during the neighboring standard measurement.

- 10 In Fig. 5c, the drift corrected and pressure and drift corrected amount fraction difference relative to the mother cylinder with respect to cylinder pressure is shown. At the point where the cell pressure started to fall below the target pressure (150 mbar [absolute](#) - Fig. 5c), the corrected data showed continuous progression, suggesting that the pressure correction is valid at that point. Towards the end of the experiment a relatively sharp increase up to 2.2 $\mu\text{mol mol}^{-1}$ was observed. **Note, however,**

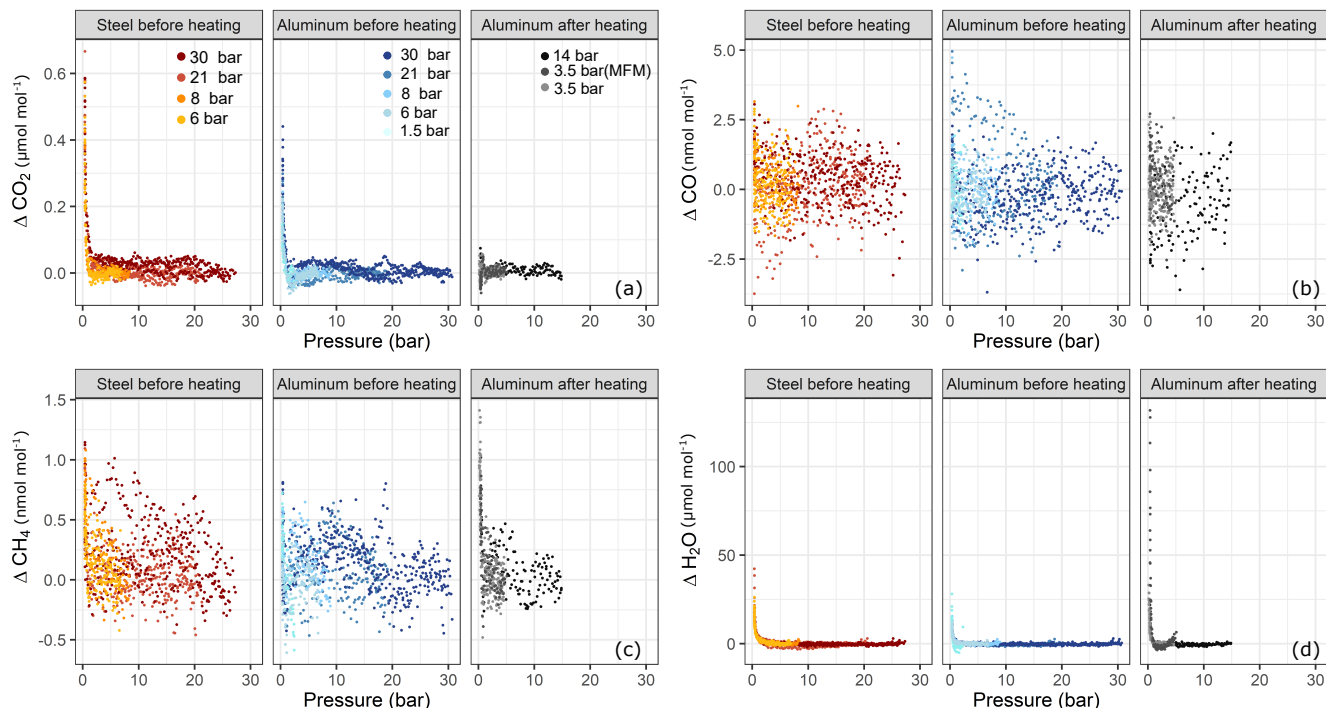


Figure 6. Amount fraction differences relative to the starting amount fractions during the course of each experiment with respect to pressure for (a) ΔCO_2 , (b) ΔCO , (c) ΔCH_4 and (d) $\Delta\text{H}_2\text{O}$. The subplots are grouped according to cylinder material and cylinder property: steel and aluminum before heating, and aluminum after heating (Table 1b-f-h). Each subplot contains a set of pressure steps denoted by different colors. Each of the colored series comprises replicates at that corresponding pressure step. x-axes show the absolute pressure values in the sample cylinder.

that-However, this increase occurred at cell pressures below 2.5 mbar, where the pressure correction function needed to be extrapolated. Also note that during the course of the experiment the volumetric flow through the analyzer amounted to no less than 3 mL min^{-1} .

However, the standard deviation of the measurements were $0.12 \mu\text{mol mol}^{-1}$ over the first 24 hours before any effect has taken over (Fig. 5c). This relatively high noise was due to the lack of sensitivity of the pressure controlling loop employed (Sec. 2.3). For the amount fraction calculations, the software uses the cell pressure reading which is more sensitive, resulting in more noisy measurements than the analyzer would achieve under its regular operation mode. Optimal parameter settings could not be found using autotuning functionality of the controller.

3.2 Experiments for filling pressure dependency using CRDS

10 In order to test for filling pressure dependency, fillings were done at various pressure levels. In Fig. 6 amount fraction differences with respect to the beginning of the experiment are plotted against the pressure in the sample cylinders. For each species,

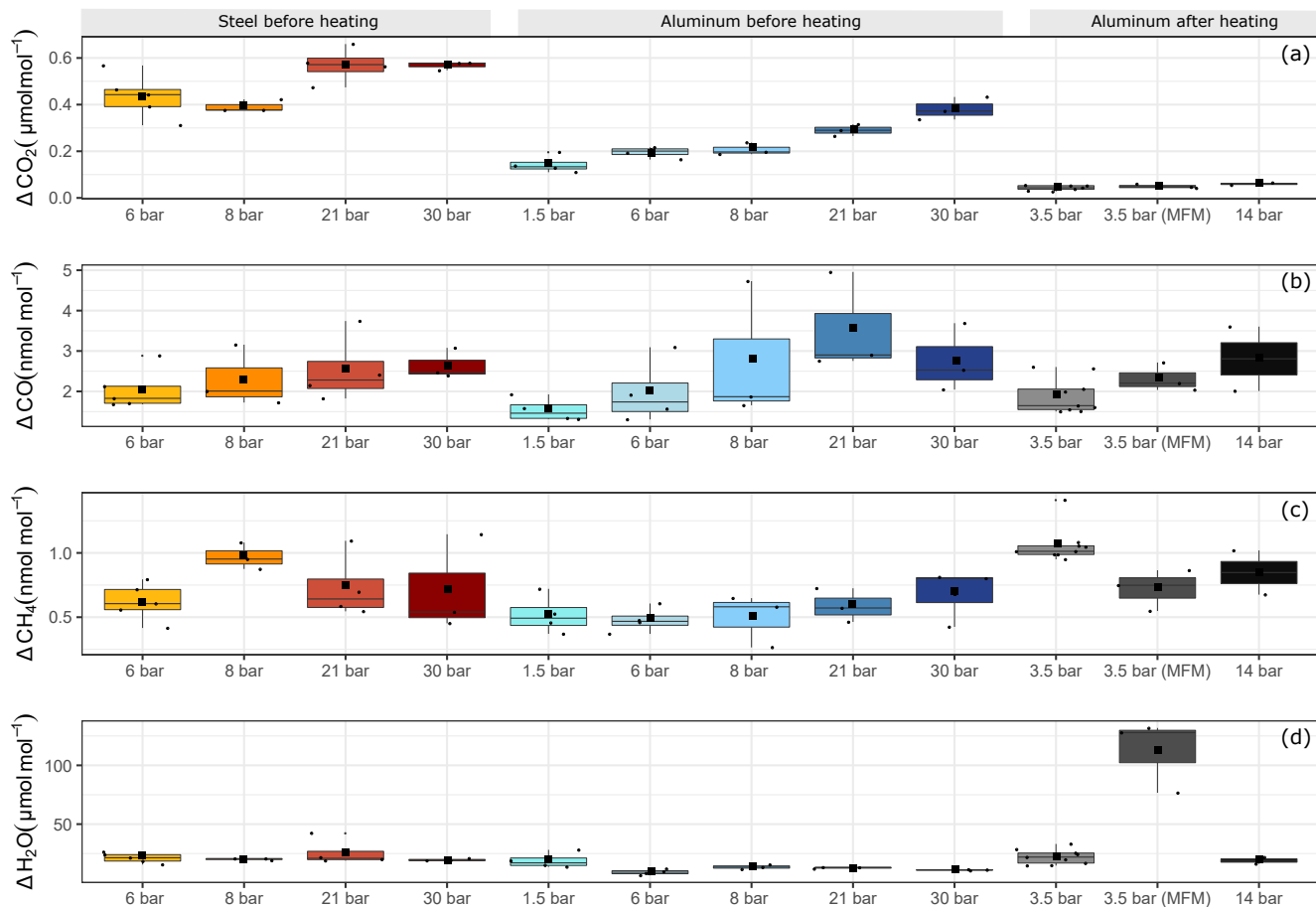


Figure 7. Filling pressure dependency of adsorption process for aluminum and steel cylinders for (a) ΔCO_2 , (b) ΔCO , (c) ΔCH_4 and (d) $\Delta \text{H}_2\text{O}$. y-axis shows the maximal amount fraction difference relative to the initial amount fraction. Each boxplot shows the mean of the maximal amount fractions of the replicates in the center of the box denoted by a square and the median is denoted by a horizontal line.

three subplots are presented, these are grouped according to cylinder material and cylinder property, namely steel before heating (Table 1b), and aluminum before (Table 1b) and after heating (Table 1f-h). Each subplot contains a set of experiments corresponding to various pressure levels. At each pressure step, there exists at least three replicates with the exception of aluminum 14 bar after heating having only two replicates. For CO_2 (Fig. 6a) and H_2O (Fig. 6d), a clear effect with decreasing cylinder pressure was observed, whereas such dependency for CO and CH_4 was very limited and not significant.

Figure 7 shows an overview of all pressure levels. Similarly to Fig. 6, we calculated the amount fraction differences from the initial amount fractions, and selected the maximal difference. This maximal difference was found in all cases towards the end of the measurements. We interpreted this enhancement as desorption of the molecules previously adsorbed to the cylinder surface. For CO_2 , the steel cylinder clearly showed higher enhancements at the end of the experiments corresponding to a mean

of $0.49 \pm 0.03 \mu\text{mol mol}^{-1}$ over the filling pressure range from 6 to 30 bar. Moreover, the aluminum cylinder showed a clear linear increase with respect to filling pressure in the final amount fractions. These corresponded to $0.14 \pm 0.02 \mu\text{mol mol}^{-1}$ and $0.38 \pm 0.03 \mu\text{mol mol}^{-1}$ for the lowest (1.5 bar) and the highest (30 bar) pressure step, respectively. This is a clear indication of physical adsorption: The higher the filling pressure, the more CO_2 molecules adsorb to the cylinder surface, and with decreasing pressure in the cylinder, CO_2 molecules leave the surface, and mix back into the gas-phase, which results in an enhancement of the measured amount fractions. The aluminum cylinder was ~~probably not yet~~ in a pressure range (up to 30 bars) where most of its available sites for adsorption were ~~saturated~~. unsaturated. This is in line with the observations of Schibig et al. (2018), which states that even at 150 bar pressure only a relatively small fraction of available adsorption sites was occupied. Changes between 30 and 150 bar seem to be minimal due to the shape of the adsorption isotherm. A linear relationship was observed with a slope of $0.01 \mu\text{mol mol}^{-1} \text{ bar}^{-1}$. However, after the second cleaning procedure (Table 1d), this behavior was no longer apparent. After heating (Sect. 3.3), the pressure effect decreased to less than $0.1 \mu\text{mol mol}^{-1}$ for CO_2 , whereas 14 bar during the initial conditions would have corresponded to $0.25 \mu\text{mol mol}^{-1}$ following the linear relationship. For measurements after heating, the aluminum cylinder showed a downwards trend in the amount fractions of CO_2 when compared to all other measurements (Supplementary material). This trend is most likely related to the time lag of the outlet valve response to decreasing pressure in the cylinder. A correction was applied to account for this effect, however the measurements still show a slight decrease of $0.05 \mu\text{mol mol}^{-1}$ which is larger than the standard deviation of the CO_2 measurements of $0.02 \mu\text{mol mol}^{-1}$. More information on this correction is presented in the Supplementary material. For all other measurements such correction was not necessary since the desorption of CO_2 overcomes the instrumental artefact.

For both cylinders over the tested pressure range, the observed surface effects were less than 5 nmol mol^{-1} and $1.5 \text{ nmol mol}^{-1}$, for the species CO (Fig. 6b) and CH_4 (Fig. 6c), respectively.

3.3 Temperature experiments with CRDS

3.3.1 Low temperature experiments (-10°C to 80°C)

In a first step, temperature effects at lower temperatures were investigated (Table 1c). In these experiments, the temperature of the climate cabinet was set from -10°C to 80°C (Sect. 2.2 and Fig. 2a). Figure 8 shows these low temperature experiments up to 80°C , where each x-axis corresponds to a temperature cycle, and the y-axis shows the amount fraction differences relative to the beginning of the experiments at 20°C . During the low temperature experiments, the changes in amount fraction were minimal. For the aluminum cylinder, temperature effects were not significant for CO_2 , CH_4 and H_2O , whereas for CO a slight step change in amount fraction was observed. The difference between 80°C and the first measurements at 20°C corresponded to 7 nmol mol^{-1} . This difference was only marginally significant compared to the standard deviation of the CO measurements of 5 nmol mol^{-1} . However, it is important to note that the increase in the amount fraction was consistent even when the cylinder was cooled down back to 20°C . In contrast to the aluminum cylinder, the steel cylinder showed higher effects for CO_2 and CO . When the cylinder was heated from 50°C to 80°C , the enhancement in the amount fraction of CO_2 and CO were $0.11 \mu\text{mol mol}^{-1}$ and 33 nmol mol^{-1} , respectively. For both species, the observed increase was five to six times higher than the

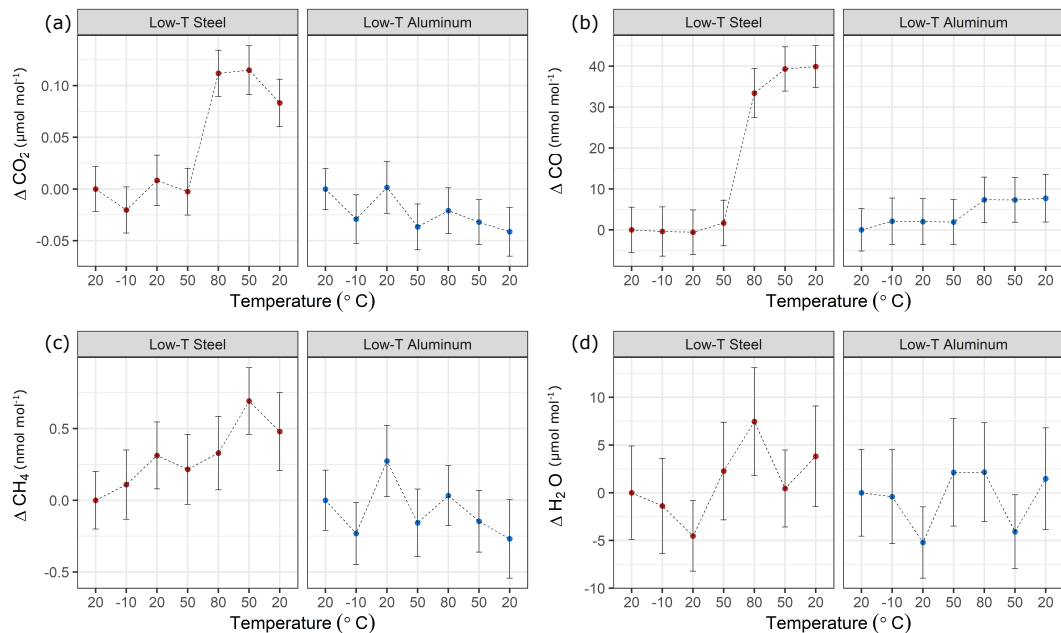


Figure 8. Temperature experiments until 80 °C using steel (red) and aluminum (blue) cylinder for species (a) CO₂, (b) CO, (c) CH₄ and (d) H₂O. x-axis corresponds to a temperature cycle, whereas the y axis shows the amount fraction differences relative to the measurements at 20 °C. Error bars indicate standard deviation of the measurements included in the mean.

standard deviation of the measurements. CO₂ showed a slight response to cooling, whereas CO amount fraction remained stable and unresponsive to cooling back to 20 °C.

3.3.2 High temperature experiments (20 °C to 180 °C)

In a further step, our aim was to understand the effects of temperature variations on cylinders to its full extent due to the discrepancy we have observed previously in big cylinders (not presented here). In order to investigate temperature effects in its extremes, we heated the cylinders up to 180 °C (Table 1c). In Fig. 9 and Fig. 10 all temperature experiments are shown. Please note that at each y-axis, the amount fractions differences relative to initial conditions at 20 °C are shown (ΔCO_2 , ΔCO , ΔCH_4 and $\Delta\text{H}_2\text{O}$). Each x-axis corresponds to temperature, and each temperature cycle is in counter clockwise direction connected by solid or dashed lines. In order to highlight the well-correlated response of the measured species, we scaled the second y-axis using the factor derived from the correlation between the species using reduced major axis regression separately for aluminum and steel cylinders. Slopes and the coefficients of determination (r^2) are given in Table 2.

During the first high temperature experiments, the steel cylinder showed enhancements as high as 21.54 $\mu\text{mol mol}^{-1}$, 16.9 nmol mol^{-1} and 4345.5 nmol mol^{-1} for CO₂, CH₄ and CO respectively. However, in the second high temperature cycle these values reduced significantly, and further decreased in the third temperature cycle amounting to 4.68 $\mu\text{mol mol}^{-1}$, 3.2

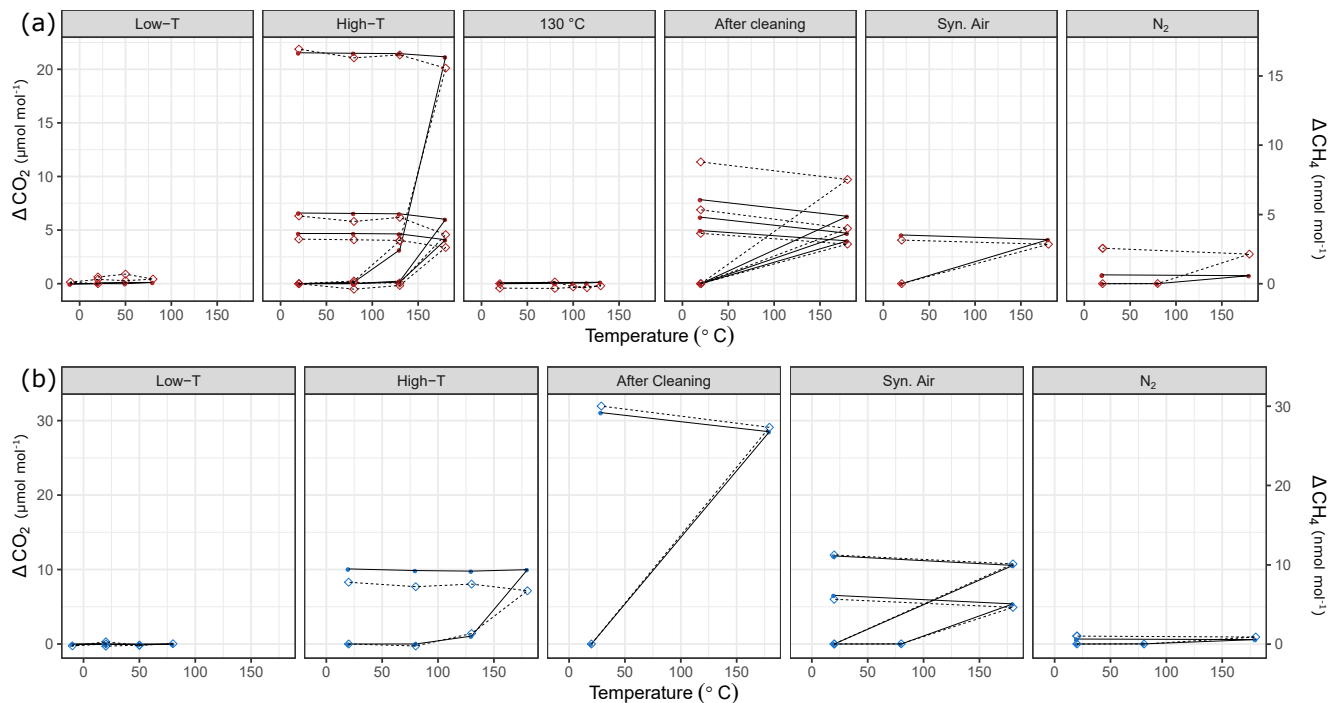


Figure 9. Temperature experiments using (a) steel (red), and (b) aluminum (blue) cylinder in chronological order for species CO₂ and CH₄. Filled circles correspond to left y-axis (CO₂), whereas open diamonds correspond to right y-axis (CH₄). See Table 1 for details of the temperature cycles. In each subplot temperature cycles are connected with solid lines for CO₂, and with dashed lines for CH₄. y-axes quantify the differences from the amount fractions measured at 20 °C (ΔCO₂ and ΔCH₄).

Table 2. Reduced major axis regression slopes and the coefficients of determination among species for temperature experiments

Cylinder	CO ₂ - CH ₄		CO - H ₂ O	
	slope	<i>r</i> ²	slope	<i>r</i> ²
Aluminum	1064.81	0.99	624.28	0.96
Steel	1292.28	0.97	815.77	0.83

nmol mol⁻¹ and 403.2 nmol mol⁻¹, for CO₂, CH₄ and CO respectively. With the exception of the first temperature cycle, the enhancements took place after 130 °C and the changes in H₂O amount fraction were reversible with temperature.

In order to highlight that these effects occurred only at higher temperatures, a temperature experiment was done up to 130 °C only for the steel cylinder (Fig. 2c). The results supported that the mechanism behind these enhancements is activated rather at temperatures higher than 130 °C. Compared to high temperature experiments (180 °C), the amount fractions increase

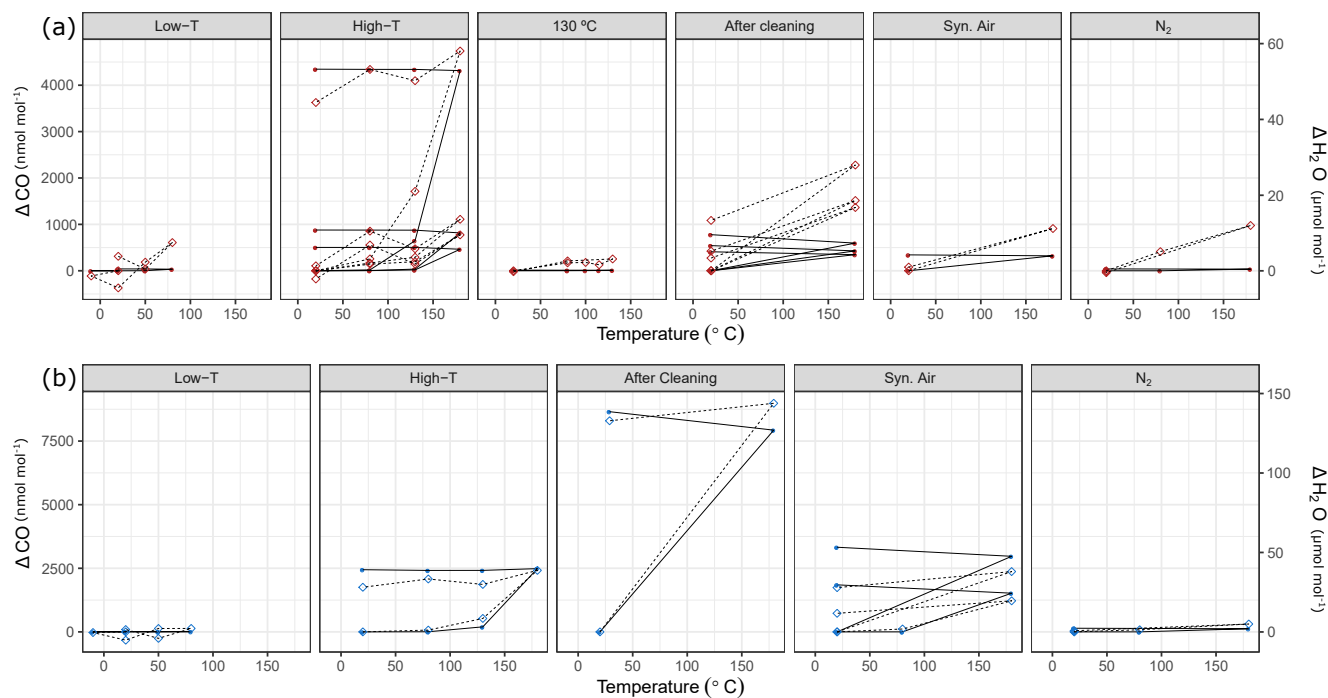


Figure 10. Temperature experiments using (a) steel (red), and (b) aluminum (blue) cylinder in chronological order for species CO and H₂O. Filled circles correspond to left y-axis (CO), whereas open diamonds correspond to right y-axis (H₂O). See Table 1 for details of the temperature cycles. In each subplot, temperature cycles are connected with solid lines for CO, and with dashed lines for H₂O. y-axes quantify the differences from the amount fractions measured at 20 °C (ΔCO and $\Delta\text{H}_2\text{O}$).

after heating until 130 °C were an order of magnitude lower being 0.1 $\mu\text{mol mol}^{-1}$ and 14.0 nmol mol^{-1} , for CO₂ and CO respectively. During the 130 °C cycle, the amount fractions of CH₄ remained unchanged, whereas H₂O showed a reversible temperature response with a slight enhancement of 3 $\mu\text{mol mol}^{-1}$ at the highest temperature. After cooling back to 20 °C, this difference was not observed anymore.

- 5 During high temperature experiments, the aluminum cylinder behaved similarly to the steel cylinder with less drastic enhancements in the amount fractions of CO₂, CH₄ and CO corresponding to 10.82 $\mu\text{mol mol}^{-1}$, 7.8 nmol mol^{-1} and 2444.1 nmol mol^{-1} . We suspected that these enhancements were related to reactions with the cleaning agent used in the ultrasonic bath (Table 1a), and it was still present on the cylinder surface. As explained in Sect. 2.2, after the first high temperature experiments, it was decided to apply a further cleaning procedure (Table 1d) for the cylinders to eliminate the traces of the cleaning
- 10 agent.

3.3.3 High temperature experiments after the second cleaning procedure (20 °C to 180 °C)

After the second cleaning procedure, the programmed temperature ramps were optimized to focus only on 20 °C and 180 °C (Fig. 2d and Table 1e), and the reversibility of the enhancements. For the steel cylinder, the applied procedure of flushing and heating did not result in a significant improvement in the amount fractions measured at 180 °C, all species were observed similarly to high temperature experiments (Sect. 3.3.2). The discrepancy between the last high temperature and first run after cleaning might be due to the steepness of the set temperature curve which might affect the mechanism of this enhancement process. However, the basic response remained unchanged, in which CO₂, CH₄ and CO showed an increase in amount fraction with decreasing intensity at each consecutive cycle, and that H₂O showed a reversible behavior.

The cleaning procedure applied on the aluminum cylinder (Table 1d) made no improvement on preventing the enhancements of the species, on the contrary, it has worsened the previous situation, amounting to differences three to four times higher: 31.07 μmol mol⁻¹, 30.0 nmol mol⁻¹, 8655.4 nmol mol⁻¹ and 132.91 μmol mol⁻¹ for CO₂, CH₄, CO and H₂O, respectively.

In order to reveal more hints of the underlying mechanism of the observed differences, several runs were done with synthetic air and N₂ (Table 1e). The fillings with synthetic air were intended to ensure that the natural compressed air used for the measurements did not include gases such as volatile organic compounds which can undergo reactions at high temperatures. The fact that both synthetic air and the compressed air filling show similar differences in amount fractions after heating to 180 °C indicates that the responsible compounds did not come from natural compressed air. In addition to the measurements with the Picarro CRDS analyzer, we sampled gas from cylinders before and after heating in the oven, and analyzed it by a Gas Chromatography with Flame-Ionization Detector technique (GC-FID) (TurboMatrix350 - Clarus500 from PerkinElmer) at the METAS Gas Laboratory. The adsorbent used was suitable for airborne C4-C8 compounds. The chromatograms showed no distinct peaks, and showed no difference between the samples before and after temperature experiments.

At a second step, the cylinders were filled with N₂ (Table 1e). A minimal difference in the amount fractions compared to all other high temperature runs were measured after the fillings with N₂. For the steel cylinder, the species CO₂, CH₄ and CO showed enhancements of 0.82 μmol mol⁻¹, 2.56 nmol mol⁻¹ and 39.7 nmol mol⁻¹, respectively. The amount fraction of H₂O was measured as 11.96 μmol mol⁻¹ at 180 °C with reversible response to heating/cooling, and thus showed a non-significant difference when cooled back to 20 °C. For the aluminum cylinder the observed differences for N₂ filling was 0.63 μmol mol⁻¹, 1.0 nmol mol⁻¹ and 143.9 nmol mol⁻¹, for CO₂, CH₄ and CO, respectively. Similar to the steel cylinder, H₂O measurements were reversible, and amounted to a maximum of 4.96 μmol mol⁻¹. However, these results should be interpreted carefully since small changes in amount fractions in very low background fractions were measured on a non-air gas matrix using the Picarro CRDS analyzer.

During the last temperature experiments (Table 1e), a temperature step between 20 °C and 180 °C was added (80 °C). This temperature will serve as an upper limit for further temperature experiments using these cylinders. When the cylinders were heated from 20 °C to 80 °C, a reversible difference of 5.1 μmol mol⁻¹ was observed only for H₂O measurements of N₂ filling for the steel cylinder. For all other species we have not observed any significant production.

The experiments with N_2 is a strong indication that the mechanism involves O_2 . This suggests combustion reactions at high temperatures under the presence of O_2 and with metal surfaces of the cylinders working as catalysts. Production of CO_2 , CO and H_2O would very well fit to complete and incomplete combustion reactions, however, the production of CH_4 cannot be reasonably explained by such reactions. The fact that all enhancements for the species are well-correlated ($r^2 > 0.8$) points toward processes of linked chemical reactions. Moreover, from our observations, it is clear that this process is irreversible with the exception of most H_2O measurements for the steel cylinder. Another possible scenario might be that, under increasing temperature, although as low as $180\text{ }^\circ\text{C}$, diffusion from the interior to the surface of the metal takes place followed by evaporation from the surface which results in enhancements in the gas phase (Smithells et al., 1935). For the steel cylinder, repeating the experiments mostly resulted in less production of amount substance which might be an indication of depletion. However, due to the lack of more detailed information, we cannot conclude which of these scenarios applies as well as the exact underlying mechanism of this process remains unclear. This investigation is beyond the scope of this study. However, these results do not prevent continuing to use these cylinders, since $180\text{ }^\circ\text{C}$ is not a typical temperature for the utilisation of gas cylinders.

4 Discussion

This study encompasses a wide range of experiments for the newly built cylinders. It is crucial to note that during these experiments, the background effect of the cylinders varied because of heating or further manipulations (Table 1d). While presenting the results, significant effort was made to highlight these changes and its chronology (Table 1). Such effects were clearly detected for the aluminum cylinder since it underwent experiments after the high temperature experiments. The results indicate that through heating, and polishing, which was applied in order to eliminate the layer formed during the ultrasonic cleaning, a more inert surface was formed. This new surface showed significantly less enhancement in the amount fraction of CO_2 .

Since we performed the experiments with a dual QCLAS system after the high temperature runs, it was only possible to compare results from the aluminum cylinder after heating. Combining the results from both analyzers, we were able to validate the applied strategy for the pressure experiments. Setting the cut-off point determined by the outlet valve parameter resulted in less than $0.1\text{ }\mu\text{mol mol}^{-1}$ enhancement in the amount fraction of CO_2 for the aluminum cylinder using the CRDS analyzer. The independent QCLAS measurements on the aluminum cylinder has not shown any effect down to [absolute](#) pressures as low as 150 mbar. Considering the $0.12\text{ }\mu\text{mol mol}^{-1}$ standard deviation of the measurements, the data from both systems are compatible with each other. Under sufficient flow rates through the cell, the measurements from the CRDS analyzer are reliable even at pressures lower than 400 mbar.

After the second cleaning procedure (Table 1d) our results compared reasonably well with the low flow experiments reported in Schibig et al. (2018) and Brewer et al. (2018). The former setup consisted of higher volume cylinders, and they suggested no difference between the coated and uncoated aluminum cylinders. The enrichment in the CO_2 amount fraction was reported as $0.090 \pm 0.009\text{ }\mu\text{mol mol}^{-1}$ (Schibig et al., 2018). On the contrary, Brewer et al. (2018) reported significant differences between the tested treated and untreated aluminum cylinders in their low flow experiments. Their results for the mixtures in untreated

aluminum cylinders with high or low water content were $0.1 \mu\text{mol mol}^{-1}$ or lower. However, it is important to note that, the previous studies used different cylinder sizes. Schibig et al. (2018) used 29.5 L cylinders, whereas Brewer et al. (2018) used 10 L cylinders corresponding to various surface to volume ratios. Moreover, these studies used different amount fractions of H_2O of $>\leq 0.05 \mu\text{mol mol}^{-1}$ and $10 \mu\text{mol mol}^{-1}$ in Brewer et al. (2018), and $>\leq 1 \mu\text{mol mol}^{-1}$ in Schibig et al. (2018). Due to its higher polarity, H_2O molecules are expected to occupy the available sites on the cylinder surface, and result in less adsorption of CO_2 molecules, which is supported by Brewer et al. (2018). Despite this varying conditions both studies did not observe effects higher than $0.1 \mu\text{mol mol}^{-1}$ at low flow conditions for untreated aluminum cylinders. On the contrary, both studies have shown effects at high flow ~~condition-conditions~~ which cannot be explained by adsorption theory alone.

A significant difference between this study and the previous studies (Leuenberger et al., 2015; Brewer et al., 2018; Schibig et al., 2018) is the onset of adsorption effects. All previous studies have shown that for high pressure cylinders, usage below 20 bar is ~~problematic-not recommended~~. This was explained through the Langmuir monolayer isotherm (Langmuir, 1918) and its exponential behavior at low pressures. ~~On the contrary~~ In contrast to the previous studies, the cylinders tested in this study showed ~~effects-enrichments~~ only well below atmospheric pressures. ~~A reason of this different evolution of the observations might be explained with the relatively~~ for the steel cylinder and the aluminum cylinder before heating. At sub atmospheric pressures, the enrichments followed a steep increase. This increase can only partly be fitted to the Langmuir adsorption isotherm if the equilibrium constant (K, the ratio between adsorption and desorption rates) are set to values higher than 1 (Supplementary material). Higher K values would correspond to higher surface coverage factors even at lower fill pressures. ~~In comparison~~ Schibig et al. (2018) have fixed the K value at 0.001 bar^{-1} , corresponding to lower surface coverage even at pressures of 150 bar. The reasonable range of the equilibrium constant remains unclear. The differences in the cylinder interior characteristics such as surface roughness or treatment is highly likely the explanation of the discrepancy in the K values. In order to understand the differences between the constructed cylinders and the Luxfer aluminum cylinder, measurements with a Luxfer cylinder of a similar size (5 L) and pressure ranges (up to 30 bar) in this study. At lower pressures, the surface coverage of would be very useful. A further investigation on the K value and modelling approaches is not within the scope of this experimental focused study.

This study also showed that the measured gases CO , CO_2 , CH_4 and H_2O had different sensitivities with respect to surface processes. We have observed surface effects for CO_2 and H_2O . Observed effects of H_2O during the pressure experiments were an order of magnitude larger than CO_2 (not shown here). One of the explanations that CO_2 and H_2O are more prone to surface effects might be due to their high boiling points. CO_2 sublimates at -78.5°C , and the boiling point of H_2O is 100°C . Whereas for CH_4 and CO , boiling points are -161°C and -191.5°C , respectively. Since CO is a reactive compound, it might be argued that it would be more prone to surface effects. However, our results have shown that CO in atmospheric air was not affected by surface interactions at short time scales (in the order of days). This is highly likely related to the ~~available-wall spaces decreases, which corresponds to adsorption of lower amount fractions. Another reason of this behavior can be that the aluminum prototype cylinder used in this study has evolved into a superior cylinder in terms of surface interactions compared to commercial cylinders. It is also worthwhile to note that the surface roughness of the presented aluminum and steel cylinders are $0.8 \leq \text{Ra} \leq 1.6$, which is presumably smoother than the commercial cylinders in use~~ competitive adsorption between species.

The ratio between the amount fraction of CO and CO₂ would be 1 to several hundreds. In order to understand competitive adsorption to its full extent, experiments focusing on a range of amount fractions would be useful. Moreover, when discussing adsorption properties, polarity is also an important criterion. Therefore, the non-polar structure of CH₄ makes it less prone to adsorption, whereas the polar geometry of H₂O enables it to be more adsorptive.

5 5 Conclusions and Outlook

We have reported the first results of the newly built cylinders which were designed to serve as chambers to investigate surface effects. The characterization of the cylinders was done under various pressure and temperature conditions, and measurement procedures were established. The rich dataset presented in this study covers the species CO₂, CO, CH₄, and H₂O using a commercial and a novel measurement device.

- 10 Pressure experiments covered a wide range from 30 bar until a few mbars. During the pressure experiments with CRDS, no effect was observed for CH₄ and CO. Prior to heating and cleaning, aluminum and steel have shown comparable adsorptive effects of 0.38 and 0.57 $\mu\text{mol mol}^{-1}$ for CO₂ for the highest fill pressure of 30 bar. The behavior of the aluminum cylinder changed after the applied procedures, corresponding to less than 0.1 $\mu\text{mol mol}^{-1}$ difference in the amount fraction between the beginning and the end of the run. The measurements from CRDS at low pressures were validated by an QCLAS system. The
- 15 results showed that for absolute pressures above 150 mbar, the enhancements in the measured amount fractions did not exceed 0.12 $\mu\text{mol mol}^{-1}$.

- The cylinders were tested at low (−10 °C to 80 °C) and high (20 °C to 180 °C) temperature ranges. Under 80 °C, both the aluminum and the steel cylinder showed limited contaminations. After temperatures of 130 °C, irreversible effects became predominant. These effects were encountered for all measured species, with the exception of H₂O during some runs. Well
- 20 correlated productions of CO₂, CH₄ and CO were observed. The most striking difference measured was as high as 8655.4 nmol mol^{−1} for CO.

- The presented measurement setup, and established procedures will further be used. Various commonly used materials will be inserted into this cylinders to test for their surface effects. Moreover, the cylinders will be used to investigate effects of other important atmospheric trace gases such as halocarbons. Additionally, the reverse process of desorption will be investigated by
- 25 using the flow through approach. Such experiments would be valuable to understand whether adsorption already occurs at very low pressures.

Appendix A

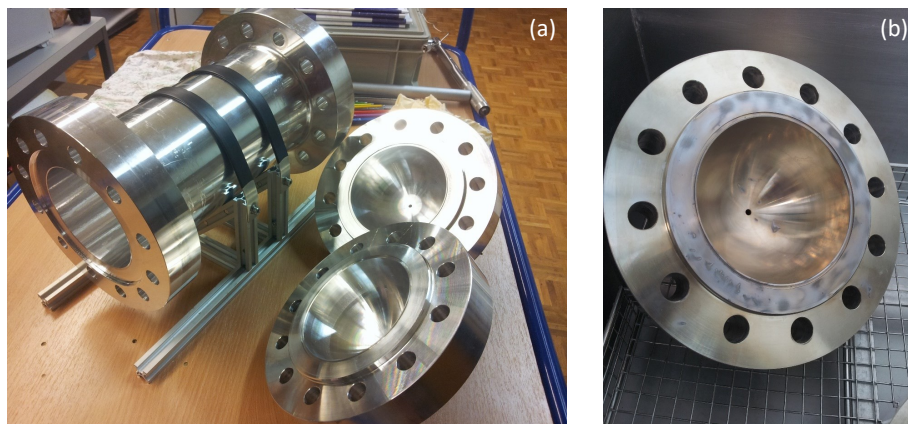


Figure A1. (a) Custom made cylinder of three pieces. (b) Stains after the ultrasonic bath during the second cleaning procedure (Table 1c).

Author contributions. ES, PN, CP, BN and ML designed the CRDS experiments. ES, PN, BB and ML designed the QCLAS experiments. ES carried out the experiments, and PN provided technical support. QCLAS measurements were carried out under the supervision of BB. ES did the data analysis and prepared the manuscript with contributions from all co-authors. ML supervised the project.

5 *Competing interests.* The authors declare that they have no conflict of interest.

Acknowledgements. This project is supported by a research contract (F-5232.30052) between the Swiss Federal Institute of Metrology (METAS) and the University of Bern. Funding for the development of the QCLAS instrument was provided by the European Research Council (ERC) under the European Union's Horizon 2020 research and innovation programme (grant agreement No 667507 (deepSLice)). The authors would like to thank to the Workshop of University of Bern for the production of the cylinders, and the METAS Gas Analysis
10 Laboratory and METAS workshop for their technical support during this work. The authors would also like to thank to Hubertus Fischer for his valuable comments on the manuscript. The authors are grateful to the members of the Laser Spectroscopy group at Empa for their support during the QCLAS measurements.

References

- Brewer, P. J., Brown, R. J. C., Resner, K. V., Hill-Pearce, R. E., Worton, D. R., Allen, N. D. C., Blakley, K. C., Benucci, D., and Ellison, M. R.: Influence of Pressure on the Composition of Gaseous Reference Materials, *Analytical Chemistry*, 90, 3490–3495, <https://doi.org/10.1021/acs.analchem.7b05309>, <https://doi.org/10.1021/acs.analchem.7b05309>, PMID: 29381338, 2018.
- 5 Keeling, R. F., Manning, A. C., Paplawsky, W. J., and Cox, A. C.: On the long-term stability of reference gases for atmospheric O₂/N₂ and CO₂ measurements, *Tellus B*, 59, 3–14, <https://doi.org/10.1111/j.1600-0889.2006.00228.x>, <https://onlinelibrary.wiley.com/doi/abs/10.1111/j.1600-0889.2006.00228.x>, 2007.
- Langenfelds, R. L., van der Schoot, M. V., Francey, R. J., Steele, L. P., Schmidt, M., and Mukai, H.: Modification of air standard composition by diffusive and surface processes, *Journal of Geophysical Research: Atmospheres*, 110, <https://doi.org/10.1029/2004JD005482>, <https://agupubs.onlinelibrary.wiley.com/doi/abs/10.1029/2004JD005482>, 2005.
- 10 Langmuir, I.: The adsorption of gases on plane surfaces of glass, mica and platinum, *Journal of the American Chemical Society*, 40, 1361–1403, <https://doi.org/10.1021/ja02242a004>, <https://doi.org/10.1021/ja02242a004>, 1918.
- Leuenberger, M. C., Schibig, M. F., and Nyfeler, P.: Gas adsorption and desorption effects on cylinders and their importance for long-term gas records, *Atmospheric Measurement Techniques*, 8, 5289–5299, <https://doi.org/10.5194/amt-8-5289-2015>, <https://www.atmos-meas-tech.net/8/5289/2015/>, 2015.
- 15 Masarie, K. A., Pétron, G., Andrews, A., Bruhwiler, L., Conway, T. J., Jacobson, A. R., Miller, J. B., Tans, P. P., Worthy, D. E., and Peters, W.: Impact of CO₂ measurement bias on CarbonTracker surface flux estimates, *Journal of Geophysical Research: Atmospheres*, 116, <https://doi.org/10.1029/2011JD016270>, <https://agupubs.onlinelibrary.wiley.com/doi/abs/10.1029/2011JD016270>, 2011.
- McManus, J. B., Zahniser, M. S., and Nelson, D. D.: Dual quantum cascade laser trace gas instrument with astigmatic Herriott cell at high pass number, *Appl. Opt.*, 50, A74–A85, <https://doi.org/10.1364/AO.50.000A74>, <http://ao.osa.org/abstract.cfm?URI=ao-50-4-A74>, 2011.
- 20 Miller, W. R., Rhoderick, G. C., and Guenther, F. R.: Investigating Adsorption/Desorption of Carbon Dioxide in Aluminum Compressed Gas Cylinders, *Analytical Chemistry*, 87, 1957–1962, <https://doi.org/10.1021/ac504351b>, <https://doi.org/10.1021/ac504351b>, PMID: 25519817, 2015.
- Nelson, D., McManus, J., Herndon, S., Zahniser, M., Tuzson, B., and Emmenegger, L.: New method for isotopic ratio measurements of atmospheric carbon dioxide using a 4.3 μm pulsed quantum cascade laser, *Applied Physics B*, 90, 301–309, <https://doi.org/10.1007/s00340-007-2894-1>, <https://doi.org/10.1007/s00340-007-2894-1>, 2008.
- 25 Pales, J. C. and Keeling, C. D.: The concentration of atmospheric carbon dioxide in Hawaii, *Journal of Geophysical Research*, 70, 6053–6076, <https://doi.org/10.1029/JZ070i024p06053>, <https://agupubs.onlinelibrary.wiley.com/doi/abs/10.1029/JZ070i024p06053>, 1965.
- Rödenbeck, C., Conway, T. J., and Langenfelds, R. L.: The effect of systematic measurement errors on atmospheric CO₂ inversions: a quantitative assessment, *Atmospheric Chemistry and Physics*, 6, 149–161, <https://doi.org/10.5194/acp-6-149-2006>, <https://www.atmos-chem-phys.net/6/149/2006/>, 2006.
- 30 Satar, E., Nyfeler, P., Pascale, C., Niederhauser, B., and Leuenberger, M.: Towards an understanding of surface effects: Testing of various materials in small volume measurement chamber and its relevance to atmospheric trace gas analysis, in preparation, 2019.
- Schibig, M. F., Kitzis, D., and Tans, P. P.: Experiments with CO₂-in-air reference gases in high-pressure aluminum cylinders, *Atmospheric Measurement Techniques*, 11, 5565–5586, <https://doi.org/10.5194/amt-11-5565-2018>, <https://www.atmos-meas-tech.net/11/5565/2018/>, 2018.
- 35

Smithells, C. J., Ransley, C. E., and Fowler, R. H.: The diffusion of gases through metals, Proceedings of the Royal Society of London. Series A - Mathematical and Physical Sciences, 150, 172–197, <https://doi.org/10.1098/rspa.1935.0095>, <https://royalsocietypublishing.org/doi/abs/10.1098/rspa.1935.0095>, 1935.

WMO: 19th WMO/IAEA Meeting of Experts on Carbon Dioxide Concentration and Related Tracers Measurement Techniques (GGMT
5 2017), Dübendorf, Switzerland, 27-31 August 2017, Tech. Rep. GAW Report No. 242, World Meteorological Organization, Geneva, Switzerland, 2018.